



PO Box 13595, Albuquerque, NM 87192 U.S.A.  
 Telephone: +1-505-220-3875  
 Email: [techinfo@fieldp.com](mailto:techinfo@fieldp.com) URL: <http://www.fieldp.com>

## Contents

1	Electron backscatter from a gold sheet	3
2	Dose from an electron beam incident on an aluminum block	9
3	Photon benchmark simulations	12
4	Angular distribution of a scattered electron beam	18
5	Electron beam energy deposition in a high-pressure gas	22
6	X-ray generation by a pinched electron-beam diode	28
7	X-ray generation from an inclined target	36
8	Pulse-height spectrum of a sodium-iodide detector	43
9	Beam passing through a thin foil	49
10	Resolution limits in X-ray radiography	53
11	Exporting power-density profiles to TDiff	60
12	Exporting power-density profiles to HeatWave	63
13	Electron backscatter at low energy	66
14	NoStepLimit function in simulations with long-range photons	68

---

# 1 Electron backscatter from a gold sheet

This introductory section gives a detailed description of a simulation to calculate the backscatter fraction for energetic electrons incident on a planar gold sheet. The simple geometry does not utilize the full resources of **GamBet** – instead, the intention is to illustrate useful techniques and the accuracy of the code. The two required input files are **BACKSCAT.MIN** (definition of the solution volume geometry) and **BACKSCAT.GIN** (specification of incident electron properties and control parameters for the Monte Carlo calculation). Move the files to a working directory. The run also accesses Penelope data files with information on the physical properties of gold. These files are located in the directory **/FIELD/GAMBET/REFERENCE**. If you encounter any problems, check the setup procedure described in the *GamBet Reference Manual*.

Figure 1 shows measurements reported in T. Tabata, R. Ito and S. Okabe, Nucl. Instrum. and Methods **94**, 509 (1971). The graph plots the backscatter ratio for gold as a function of the kinetic energy of electrons at normal incidence. The small black circles are data points, while the line represents the best fit. The backscatter ratio is the number of electrons that emerge from the front face divided by the number of incident electrons assuming that the foil is thick enough so that there are no transmitted electrons. In our simulation we shall check the ratio at energies of 1.0, 3.0 and 10.0 MeV. To plan the run we need information on electron ranges in gold. The following Internet site is a useful source of information:

<http://physics.nist.gov/PhysRefData/Star/Text/ESTAR.html>

The interactive site gives information on the interactions of energetic electrons with matter including the total range. The first data column of Table 3 shows the EStar results.

The planar 2D approximation applies when the transverse dimension of the sheet is large compared to the extent of the incident beam and backscattered electrons. We assume that electrons initially move in the  $+x$  direction. The script to define the geometry mesh is shown in Table 1. The solution volume consists of a single material region with 0.5 cm thickness in the  $x$  direction. The depth is sufficient to prevent electron loss by transmission at the highest energy. Electrons that leave the solution volume are included in run statistics and the particle escape file. We shall use this information to determine the backscatter ratio. The mesh has variable resolution in  $x$  with small elements near the entrance at  $x = 0.0$  cm. The element division could be used to study dose distributions for electrons of different energies. The element size is not critical for the backscatter calculation. A mesh with a single layer of elements in  $x$  would yield the same accuracy with little difference in run speed. The system has dimensions  $\pm 0.3$  cm in the  $y$  direction. The width is sufficient to ensure that scattered electrons are not lost from the top and bottom boundaries. The first step in the run is the creation of the geometry input file **BACKSCAT.MOU**. Start **GBLaunch** and check that the data directory points to the working directory. Start the **Mesh** program, click on **File/Load script (MIN)**, choose **BACKSCAT.MIN** and click **OK**. Choose the **Process** command to generate the mesh and then click on **File/Save mesh (MOU)**.

Table 2 shows the contents of the file **BACKSCAT.GIN**. The **GFile2D** command of the **Geometry** section directs **GamBet** to load node and element information from **BACKSCAT.MOU** and to interpret the system as planar (variations in  $x$  and  $y$  with infinite length in  $z$ ). The **DUnit** command

Table 1: File BACKSCAT.MIN to create the geometry file

```

* File: BACKSCAT.MIN
* Dimensions in cm
* -----
GLOBAL
  XMESH
    0.000  0.100  0.002
    0.100  0.500  0.010
  END
  YMESH
    -0.300  0.300  0.010
  END
END
* -----
REGION  FILL SolnVolume
  L      0.00 -0.30  0.50 -0.30
  L      0.50 -0.30  0.50  0.30
  L      0.50  0.30  0.00  0.30
  L      0.00  0.30  0.00 -0.30
END
* -----
ENDFILE

```

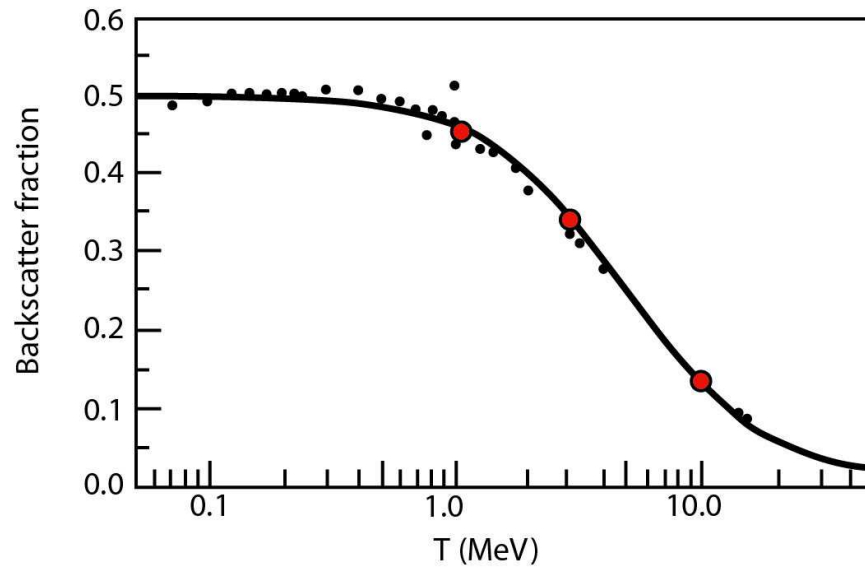


Figure 1: Electron backscatter from a gold foil, comparing experimental results and **GamBet** calculations

Table 2: File BACKSCAT.GIN to control the **GamBet** calculation

```
* File: BACKSCAT.GIN
GEOMETRY
  DUnit 100.0
  GFile2D BackScat.MOU  Rect
END
COMPOSITION
  Material 79
  Region(1) = 1
END
SOURCE
  SList
    E 1.0E6 0.0001 0.00 0.00 1.00 0.00 0.00
*   E 3.0E6 0.0001 0.00 0.00 1.00 0.00 0.00
*   E 10.0E6 0.0001 0.00 0.00 1.00 0.00 0.00
  End
  NPMult = 50000
END
PROCESS
  EAbs Electron 1.0E5
  EAbs Photon 1.0E5
  EAbs Positron 1.0E5
  C1 0.10
  C2 0.10
  WCc 1.0E5
  WCr 1.0E5
  PlotOn 50
END
ENDFILE
```

specifies that coordinate dimensions are in centimeters. The commands of the **Composition** section define Material 1 as gold ( $Z = 79$ ) and associates Region 1 (the complete solution volume) with the material. The **SList** command in the **Source** section lists a single primary electron with kinetic energy 1.0 MeV moving in the  $+x$  direction. Notice that the start position (0.0001, 0.0, 0.0) is just inside the solution volume close the left boundary. The position ensures that **GamBet** will find a valid element within the geometry mesh to start the particle orbits. There are three lines for the energies that we shall study – two of the lines are deactivated with comment symbols. The **NPMult** command instructs the program to generate 50,000 showers (instances of the primary particle) for good statistics. Finally, the commands of the **Process** section control the Monte Carlo calculation. A cutoff energy of 100 keV is applied to all types of particles. The value is also used for the parameters  $W_{cc}$  and  $W_{cr}$  (transition energies between continuous and discrete calculations). The value is high enough to ensure fast calculations but relatively low compared to initial electron energy. The final **PlotOn** command instructs **GamBet** to generate a plot file of primary and secondary particle orbits for 50 showers.

Run **GamBet** from **GBLaunch**, click on **Run/Start run** and choose **BACKSCAT.GIN**. Following the script instructions, the program loads information on geometry and material properties and then begins the Monte Carlo simulation for 1.0 MeV electrons. The run with 50,000 showers takes about 57 seconds on a 3.4 GHz computer. Upon completion **GamBet** displays two important pieces of status information. The programs states that no particle histories terminated early because they exceeded *NStep* and displays the energy conservation factor. The quantity equals the difference between the energy input and the sum of deposited and escape energies divided by the input energy. The factor should be small compared to unity – for this run it equals about 0.025%.

The listing file contains the primary information for the backscatter calculation. Click on **File/Edit listing files**, choose **BACKSCAT.GLS** and click **OK**. **GamBet** opens the file in its internal editor. The first section of the listing file records input parameters and details of the run setup. The run statistics section (near the end of file) contains the following information:

```
Primary electrons
Escape fraction:      0.4479
Average energy of escape electrons:  7.1946E+05 (eV)
Average pathlength of escape electrons:  1.3761E-02 (cm)
Average pathlength of absorbed electrons:  3.9575E-02 (cm)
```

The code predicts that 44.8% of primary electrons leave the solution volume with average kinetic energy of 0.7194 MeV after traveling an average distance of 0.0138 cm through the material. Because particles can leave only through the front face, the escape fraction equals the backscatter fraction for primary electrons. The average pathlength for absorbed electrons is 0.0396 cm, close to the EStar range value. The backscatter fraction of primary electrons is not exactly equal to the experimental results which include the contribution of knock-on electrons. The region flux listing (shown below) gives the total number of electrons that leave the solution volume per incident primary particle. The energy flux is the energy crossing the region boundary per incident primary. Therefore, the average energy of all electrons leaving the front face of the solution volume is  $324.3/0.4607 = 703.9$  keV.

```
--- Region fluxes ---
  NReg  NReg  Electron  Electron
  From  To    flux      eng. flux
                (p/p)      (eV/p)
=====
    1    0  4.607000E-01  3.243001E+05
```

Table 3 lists values of the primary and total backscatter fraction for energies of 1.0, 3.0 and 10.0 MeV. **GamBet** calculations of the total backscatter fraction are plotted as red circles in Fig. 1. The values are quite close to the experimental result.

During the course of a run **GamBet** records extensive information on the orbits and dose distribution. Run **GBView2** from **GBLaunch**. Click on **File/Load dose file** and choose **BACKSCAT.G2D**. The program loads information and creates a default dose plot. To add orbits, click on **File/Load trajectories** and choose **BACKSCAT.GPL**. Figure 2 shows trajectories of 1.0 MeV electrons. In order to replicate the plot, use the **Spatial plots/Zoom window** command to narrow the view. Dose information is not particularly useful in the present calculation

Table 3: Backscatter example results

Energy (MeV)	Range (cm)	Primary fraction	Total fraction
1.0	0.0402	0.449	0.461
3.0	0.1228	0.317	0.331
10.0	0.3185	0.113	0.139

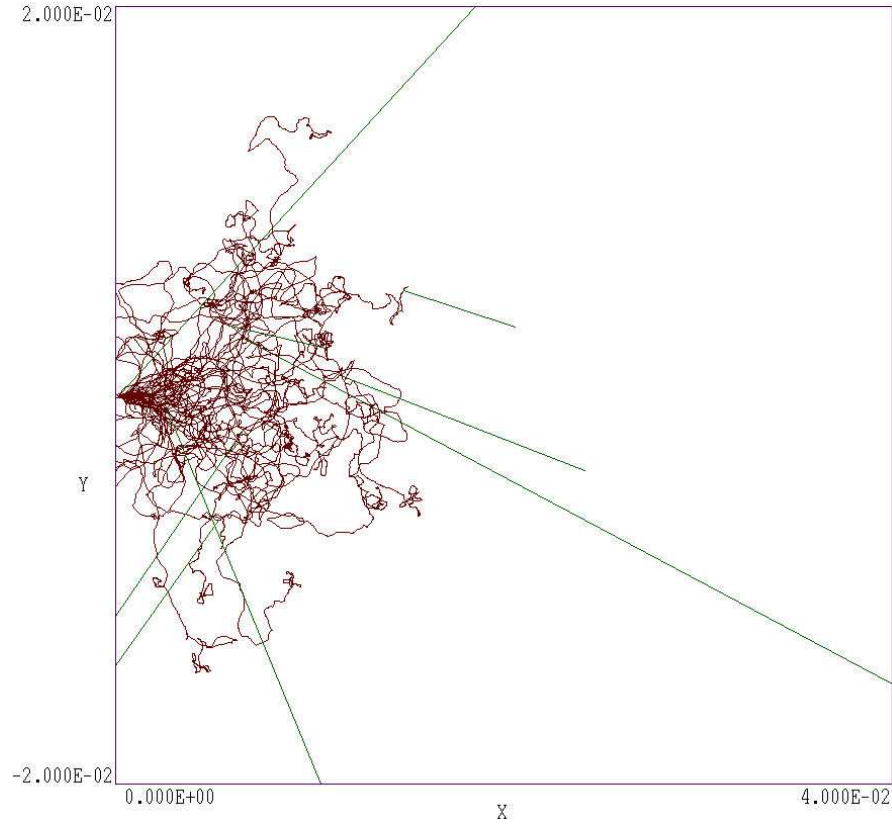


Figure 2: Representative orbits for electrons incident at 1.0 MeV, zoomed view of the entrance region. Brown: primary and secondary electrons. Green: photons.



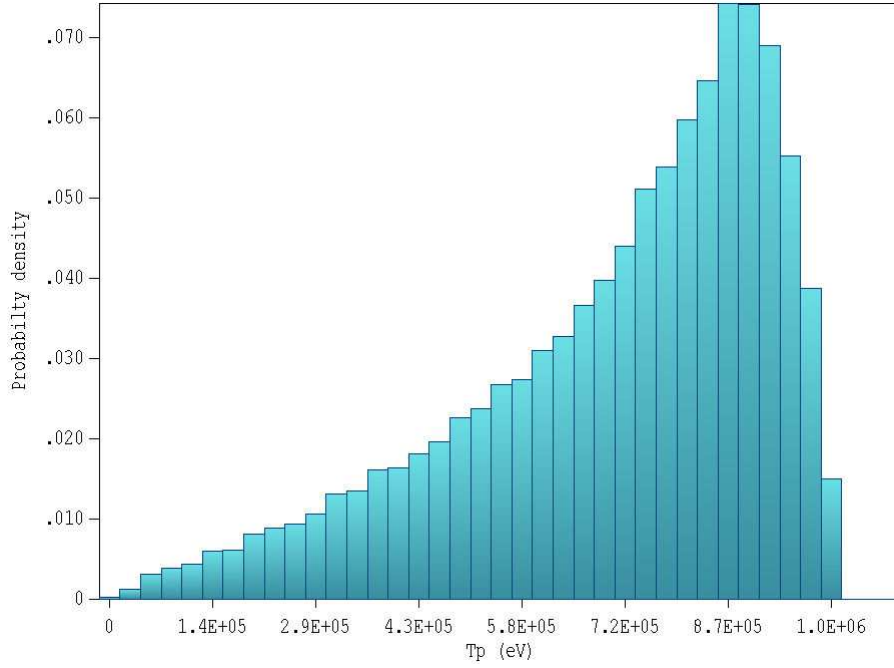


Figure 3: Energy distribution of electrons escaping through the front face of the solution volume.

because of the relatively large element size and the spatial singularity of the input distribution. Therefore, click on **Spatial plots/Plot type** and uncheck the **Dose** box in the dialog. In this case, the dose file is used only to supply boundaries for the plot.

You can use the **GenDist** program to analyze the distribution of particles contained in the escape file. Run the program and choose the command **File (SRC/PRT)/Load SRC** and choose **BACKSCATESC.SRC**. Figure 3 shows a plot of the relative number of electrons leaving the front face of the solution volume in terms of kinetic energy for an incident energy of 1.0 MeV. The following operations were used to create the plot. Click on **Plot/Plot type** and choose **1D Bins**. In the dialog initiated by *Plot/Plot quantity* choose  $f(T)$ . To ensure that the plot contains only electrons leaving the front face, click on **Analysis/Apply filter**. In the dialog, check the radio button for electrons and set  $XMax = 0.001$  and  $UxMax = 0.0$ . Finally, choose the command **Plot/Plot limits**. Uncheck the *Autoscale* option for kinetic energy and supply the values 0.0 and  $1.1 \times 10^6$ .



## 2 Dose from an electron beam incident on an aluminum block

The calculation discussed in this tutorial treats a 1 MeV sheet electron beam incident on an aluminum block. The calculation has two goals:

1. Demonstrate how to define an incident electron beam.
2. Show how to interpret dose units in **GamBet** and **GBView2**.

The two required input files are `ALUMBEAM.MIN` and `ALUMBEAM.GIN`. The simple planar 2D system consists of an aluminum block of thickness 0.20 cm in the beam direction. The beam has a height  $h = 0.11$  cm and the solution volume extends from  $y = -0.15$  cm to 0.15 cm in this direction. The mesh element size is about 0.01 cm.

The first step in planning the simulation is to consult the EStar database at:

<http://physics.nist.gov/PhysRefData/Star/Text/ESTAR.html>

The site lists the following information on the interactions of 1 MeV electrons with aluminum (density  $\rho = 2.6989$  gm/cm<sup>3</sup>).

ESTAR: Stopping Powers and Range Tables for Electrons						
ALUMINUM						
Kinetic Energy	Collision Stp.	Radiative Stp.	Total Stp.	CSDA Range	Radiation Yield	
MeV	MeV	cm2/g	MeV	cm2/g	MeV	cm2/g
=====						
1.000E+00	1.465E+00	2.119E-02	1.486E+00	5.546E-01	7.636E-03	

The physical range is 0.205 cm. Therefore, the aluminum slab is sufficiently thick to stop the strongly-scattered distribution of electrons.

The incident sheet beam is represented by 21 primary particles with a uniform spacing of 0.05 cm along  $y$ . Table 4 contains an extract from the *SList* structure of `ALUMBEAM.GIN` showing some of the particle data lines. All particles start just inside the left-hand boundary of the slab and move in the  $+x$  direction. The run includes 500 showers for each primary for good dose statistics. Each primary particle carries  $1.0 \times 10^{-4}$  A/m of current, so the linear current of the beam is  $J = 2.1 \times 10^{-3}$  A/m. The average beam current density is therefore  $j = J/h = 1.909$  A/m<sup>2</sup>. Ignoring the contributions of backscattered electrodes, the dose rate at the slab entrance can be calculated from the EStar total stopping power,  $S = 4.01 \times 10^8$  eV/m. The dose rate is given by

$$D = \frac{Sj}{\rho} = 2.836 \times 10^5 \text{ Gy/s.}$$

Note that the SI unit of dose is the Gray, where 1 Gy = 1 J/kg.

Table 4: Source section from the file ALUMBEAM.GIN

```

SOURCE
SList
  E  1.0E6 0.0001  0.050 0.00  1.00 0.00 0.00  1.0E-4
  E  1.0E6 0.0001  0.045 0.00  1.00 0.00 0.00  1.0E-4
  E  1.0E6 0.0001  0.040 0.00  1.00 0.00 0.00  1.0E-4
  ...
  E  1.0E6 0.0001 -0.045 0.00  1.00 0.00 0.00  1.0E-4
  E  1.0E6 0.0001 -0.050 0.00  1.00 0.00 0.00  1.0E-4
End
NPMult = 500
END

```

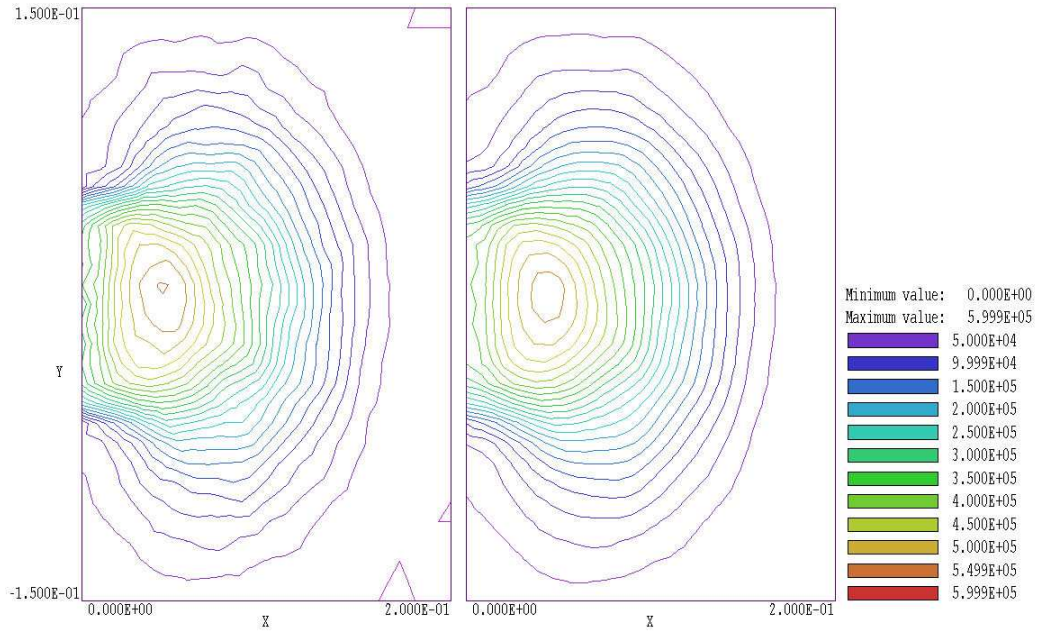


Figure 4: Dose rate distribution from an electron beam striking an aluminum block. Beam properties:  $T = 1.0$  MeV,  $h = 0.11$  cm and  $J = 2.1 \times 10^{-3}$  A/m. Left: raw data. Right: Smoothed data.

The files `ALUMBEAM.GLS` and `ALUMBEAM.G2D` are created by running **Mesh** and then **GamBet**. Running **GBView2** and loading `ALUMBEAM.G2D` gives the default contour plot of dose rate in the  $x$ - $y$  plane shown on the left-hand side of Fig. 4. Inspection of the figure shows that the dose rate at the entrance face is close to the theoretical value. The **GamBet** calculation is slightly higher because of power deposition by backscattered electrons. The dose rate is enhanced at a depth of about 0.05 cm because of the effect of electron scattering in the  $z$  direction. The electrons fan out and deposit energy over a tree-shaped region with size comparable to the electron range. The effect of statistical variations of deposited power between the small element is visible in the figure. Smoothing the distribution is equivalent to increasing element size – statical noise is reduced at the expense of some loss of resolution. The right-hand side of Fig. 4 shows the modified dose distribution after one application of the *Smooth Dose* command in **GBView2**.

To conclude, we can check **GamBet** calculations of flux through region boundaries for a planar geometry in the continuous beam mode. The code predicts a backscatter ratio for primary electrons striking aluminum of 0.1094. The average energy of the backscattered primaries is 429.9 keV. With the beam linear current  $J = 2.1 \times 10^3$  A/m, the expected return energy flux through the front face of the slab is 98.8 J/s/m. The value reported in the region flux table of `ALUMBEAM.GLS` for power flow from Region 1 to Region 0 is 100.0 J/s/m. The value is slightly higher because of the contribution of secondary electrons.

---

### 3 Photon benchmark simulations

This tutorial discuss two simulations of gamma ray generation and transport in a lead slab. The intention is to show useful **GamBet** techniques and diagnostic capabilities in **GBView2** and **GenDist**. The simple planar 2D geometry facilitates comparison to theory.

In the first example, 1.0 MeV gamma rays strike a lead slab (1.0 cm thickness) at normal incidence. The calculation demonstrates some capabilities for distribution analysis in **GenDist**. The input files are **LEADSLAB.MIN** and **LEADSLAB.GIN**. The geometry file defines a single region with length 1.0 cm along  $x$  and height  $\pm 5.0$  cm along  $y$ . The large extent in  $y$  and infinite width in  $z$  ensure that no photons are lost through the transverse faces. The goal of the calculation is to find the total attenuation coefficient  $\mu$ . The parameter gives the fractional flux of full-energy photons that emerge from a target of thickness  $L$  through the equation:

$$F(L)/F_0 = \exp(-\mu L).$$

The strategy is to initiate 10,000 showers and to record the parameters of particles that leave the solution volume in the escape file **LEADSLABESC.SRC**. The file is then loaded into **GB**. A filter is added to restrict particles to full-energy photons that exit the downstream face. A modified **SRC** file is generated and reloaded to count the particles included in the filtered class.

We use the NIST XCom site to find quantities for a theoretical comparison. The site, located at

<http://physics.nist.gov/PhysRefData/Xcom/Text/XCOM.html>

is an invaluable resource for planning runs involving photons. XCom generates graphs and listings of attenuation coefficients for coherent and incoherent scattering, photoelectric absorption and pair production. Figure 5 illustrates an XCom plot. The site provides the following values for the normalized total attenuation coefficient for 1.0 MeV gamma rays in lead:  $\mu_n = 0.071 \text{ cm}^2/\text{gm}$  with coherent scattering and  $\mu_n = 0.068 \text{ cm}^2/\text{gm}$  without coherent scattering. The process of *coherent scattering* changes the direction of photons but not their energy. Because we do not intend to filter by angle, we use the value of  $\mu_n$  that does not include coherent scattering. Multiplication by density of lead ( $\rho = 11.35 \text{ gm/cm}^3$ ) gives the total attenuation coefficient:

$$\mu = \rho\mu_n = (0.068)(11.35) = 0.772 \text{ cm}^{-1}.$$

Inserting the value in the previous equation with  $L = 1.0 \text{ cm}$ , we find that  $F(x)/F_0 = 0.462$ .

To carry out the calculation, run **Mesh** and **GamBet** to create the file **LEADSLABESC.SRC**. Run **GenDist**, pick the command **File (PRT/SRC)/Load SRC file** and choose the file in the dialog. Next, click on the command **Analysis/Apply filter**. In the dialog, activate the **Photon** radio button and enter the values 0.9 for **XMin** and  $0.99 \times 10^6$  for **KEngMin**. Click **OK** to continue. The filter eliminates knock-on electrons and backscattered or reduced-energy photons. Choose the command **File (PRT/SRC)/Write PRT/SRC file** and supply the prefix **LEADSLABMOD**. Return to the main menu and load the new source file. The information dialog

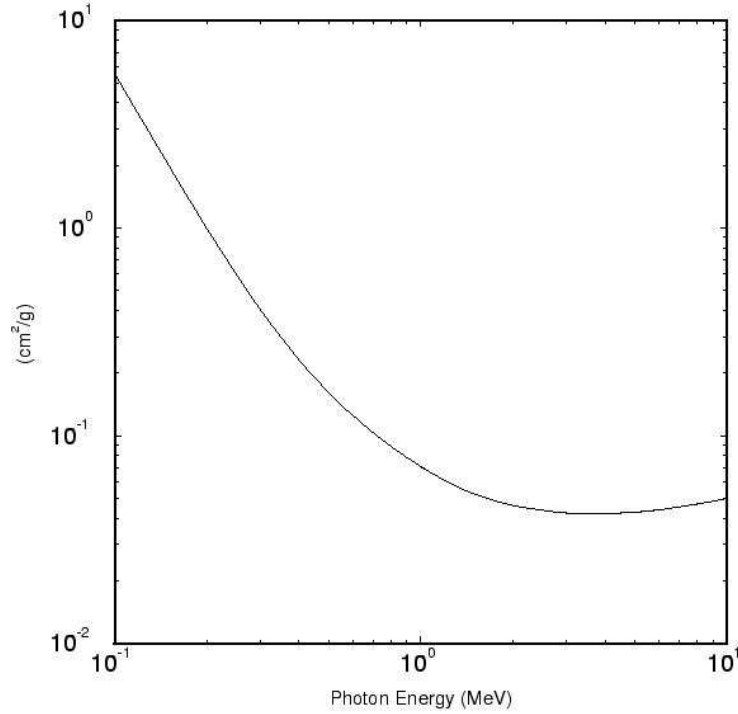


Figure 5: Total attenuation coefficient (with coherent scattering) for gamma rays in lead. Data generated by the NIST XCom site.

shows that the file contains 4602 particles. The implied value  $F(L)/F_0 = 0.460$  is in good agreement with the prediction.

As a final activity, we shall generate a plot of the transverse distribution of scattered photons at the downstream face of the slab. Reload `LEADSLABESC.SRC` into **GenDist** and return to the **Apply filter** dialog. Leave the constraints on particle type and *XMin* in place, but remove the filter on kinetic energy. Set the plot type to Spatial projection and the plot quantity to *Y-Z*. In the default *AutoScale* mode, a few photons with large angles give a skewed plot with a large field of view. To improve the appearance of the plot, click on **Plot/Plot limits** to bring up a dialog. The active fields depend on the type of distribution plot. In this case, uncheck the *AutoScale* boxes and supply limits for the *Y* and *Z* axes. Figure 6 was generated with the choices *YMin* = -1.25, *YMax* = 1.25, *ZMin* = -1.25 and *ZMax* = 1.25.

The second example treats generation of bremsstrahlung radiation by an electron beam striking a thin target. The calculation demonstrates interaction forcing to improve output statistics. The input files are `BREMSFORCE.MIN` and `BREMSFORCE.GIN`. A 5.0 MeV electron beam is normally incident on a lead sheet of thickness 0.324 mm in *x* with extents  $\pm 0.150$  mm in *y*. The sheet thickness is about 1/10 the electron range, so we can make approximate comparisons to theory. The following information for 5.0 MeV electrons in lead was generated by the NIST EStar site:

Kinetic Energy MeV	Collision Stp. MeV	Radiative Stp. cm2/g	Total Stp. cm2/g	CSDA Range g/cm2	Radiation Yield
5.000E+00	1.120E+00	5.773E-01	1.698E+00	3.673E+00	2.045E-01

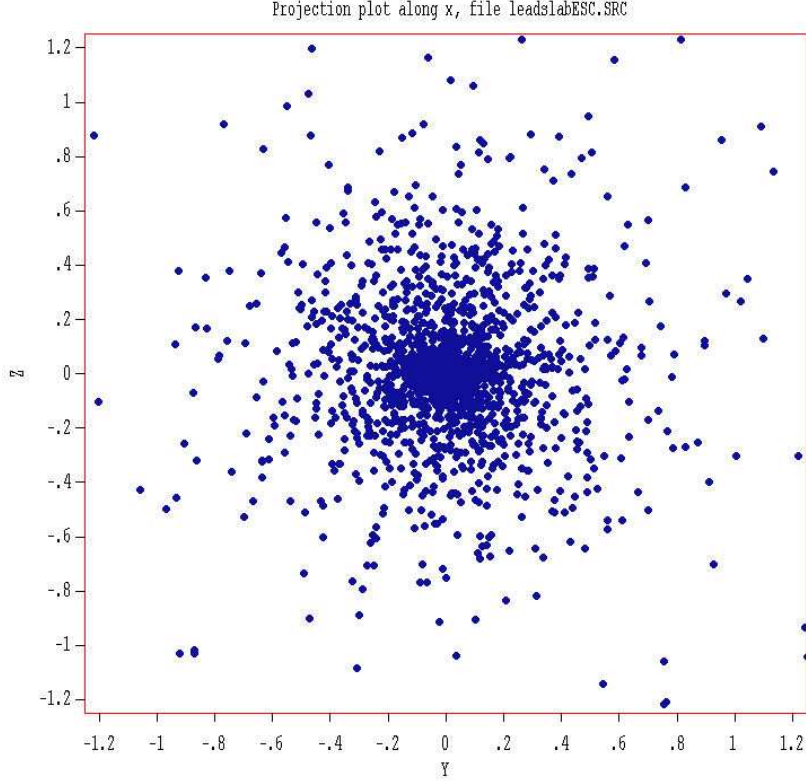


Figure 6: Example LEADSLAB – transverse spatial distribution of photons at the exit plane.

Table 5 shows the **GamBet** control script BREMSFORCE.GIN. The cutoff energies are set to 50.0 keV to give a short run time. As a result, the spectrum of escaping gamma rays will contain no data for lower energies. An initial run was performed without interaction forcing. There were 20,000 injected electrons. Because the probability of bremsstrahlung interactions was low compared to scattering and collisional energy loss, the escape file contained only 6279 photons. The top plot in Fig. 7 of the energy spectrum of downstream photons shows a high level of statistical noise. The plot was created with **GenDist** with the following options: 1) the plot type is *1D Bins*, 2) the plot quantity is *T* and 3) energy weighting is applied. With energy weighting, the vertical axis shows the relative photon energy-flux per kinetic-energy interval.

The statistical variations of output quantities can be significantly reduced by adding the command

```
Force Brems 50.0
```

In this case, **GamBet** raises the probability of bremsstrahlung interactions by 50.0 but reduces the energy-deposition weight of resulting photons by a factor of 0.02. This technique increases the number of bremsstrahlung photons but ensures that their effect on materials in the solution volume is unchanged. With interaction forcing, the total number of photons in the escape file increases to 288708. The statistical improvement is evident in the bottom plot of Fig. 7. The run time is 59 s. Although the number of photons increased by a factor of 50, the run time rose by only a factor of 2.7. **GamBet** performs much less work tracking photons (which undergo only discrete interactions) than electrons. Therefore interaction forcing is highly effective in modeling bremsstrahlung targets.

Table 5: Control script BREMSFORCE.GIN

```

GEOMETRY
  DUnit 1000.0
  GFile2D BREMSFORCE.MOU Rect
END
COMPOSITION
  Material Pb
  Region(1) = 1
END
SOURCE
  SList
    E 5.0E6 0.00001 0.00 0.00 1.00 0.00 0.00
  End
  NPMult = 20000
END
PROCESS
  EAbs Electron 5.0E4
  EAbs Photon 5.0E4
  EAbs Positron 5.0E4
  C1 0.10
  C2 0.10
  WCc 5.0E4
  WCr -5.0E4
  DsMax(1) = 0.01
  Force Brems 50.0
  NoStepLimit
END
ENDFILE

```



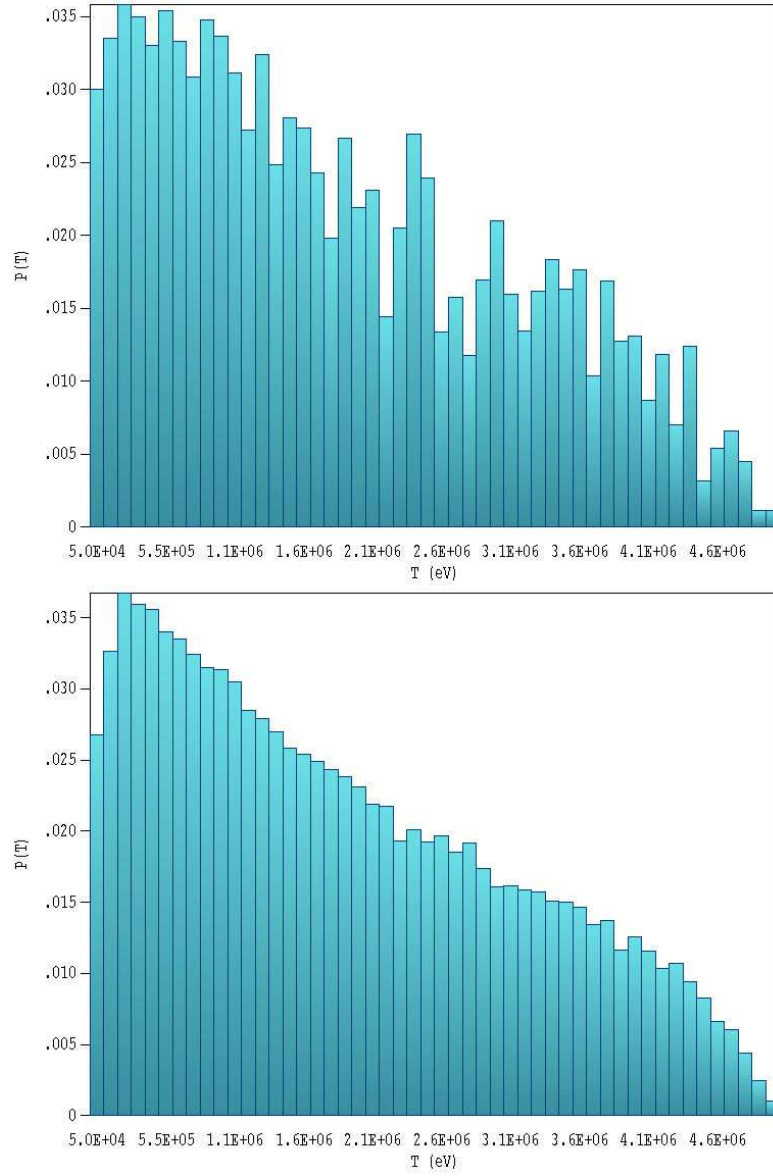


Figure 7: Bremsstrahlung photon relative energy flux as a function of kinetic energy, example BREMSFORCE. Top: Without interaction forcing. Bottom: With interaction forcing.

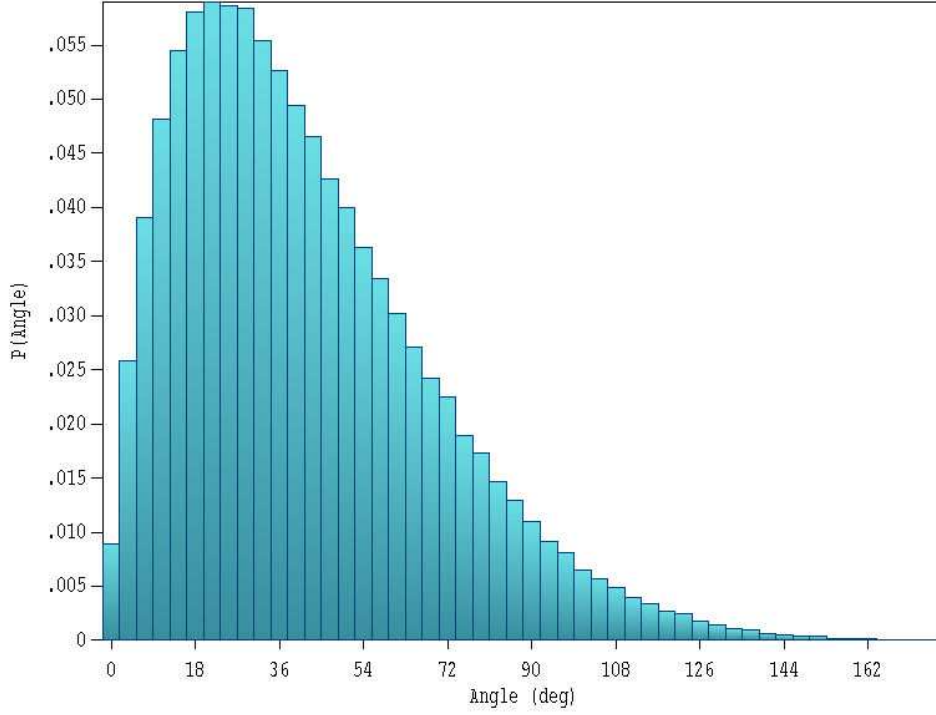


Figure 8: Bremsstrahlung photon relative energy flux as a function of angle with respect to the electron beam axis, example BREMSFORCE.

To conclude, we can make some other comparisons of code results to theory. Using the total stopping power from the EStar data, the predicted change in electron kinetic energy is

$$\Delta T_e \cong -(1.698 \text{ MeV-cm}^2/\text{g}) (11.350 \text{ g/cm}^3) (0.034 \text{ cm}) = 0.655 \text{ MeV}.$$

The predicted average electron energy at the downstream boundary of the sheet is 4.345 MeV. The radiative stopping power value implies that the average energy lost to photons by an incident electron is

$$\Delta T_e \cong -(0.577 \text{ MeV-cm}^2/\text{g}) (11.35 \text{ g/cm}^3) (0.034 \text{ cm}) = 0.223 \text{ MeV}.$$

For comparison the following entries appear in the file BREMSFORCE.GLS:

```
Average input energy: 5.0 MeV
Average output electron energy: 4.310 MeV
Average energy lost to photons per primary: 0.231 MeV
```

The output energy is slightly lower than the prediction because of elongation of electron paths by small-angle scattering. The code gives a thin-target radiation conversion efficiency of 4.6%. Figure 8 shows a plot generated by **GenDist** of the angular distribution of forward-directed bremsstrahlung photons.

---

## 4 Angular distribution of a scattered electron beam

In this tutorial, we will determine the exit angular distribution of an electron beam passing through a metal foil. One purpose of the calculation is to check the accuracy of **GamBet** 3.0/**Penelope** 2006, comparing results to experiments and other codes. A second is to show how to find angular dispersion with **GenDist**.

A recent paper<sup>1</sup> compares electron scattering predictions of the Monte Carlo libraries **Penelope**, **Geant**, **EGNSRC** and **MCNPX** with experimental results. The paper reviews several examples – in this tutorial we shall concentrate on a 2.25 MeV electron beam passing through an aluminum foil with normalized thickness 0.0266 gm/cm<sup>2</sup>. Using the **View material file** command in the **GamBet File** menu, we find that **Penelope** uses an aluminum density of 2.6989 gm/cm<sup>3</sup>. The physical thickness of the foil is therefore  $9.863 \times 10^{-3}$  cm or 98.63  $\mu$ m.

At small angles, the distribution of the forward flux of electrons scattered in a thin foil follows the distribution

$$p(\theta) = p(0) \exp\left(-\frac{\theta^2}{\theta_e^2}\right), \quad (1)$$

where  $\theta$  is the trajectory angle with respect to the  $z$  axis and  $p(\theta)$  is the probability density (the particle intensity per steradian). The quantity  $\theta_e$  is the angle at which the intensity drops to  $(1/e)$  of its on-axis value. The experimental result for the aluminum foil quoted in the Vilches paper is  $\theta_e = 9.5^\circ$ .

Both two- and three-dimensional **GamBet** solutions (**ALUMSCAT2D**, **ALUMSCAT3D**) were run for comparison – they produced identical results. This tutorial reviews the two-dimensional setup. In the cylindrically-symmetric solution, the mesh consists of a single region representing aluminum that extends from 0.0  $\mu$ m to 98.63  $\mu$ m along  $z$  and to a maximum radius of 100.0  $\mu$ m. The large outer radius allowed collection of strongly scattered electrons in the exit plane. Table 6 lists the **GamBet** control script for the run. The **DUNIT** command signals that the **Mesh** file has units of  $\mu$ m. The **SLIST** command defines a single primary particle corresponding to a thin beam moving along the axis. Note that the initial  $r$  and  $z$  positions have been slightly shifted from zero to ensure that showers begin within the aluminum volume. The value of **NpMult** specifies that each process creates 100,000 showers. The **PARALLEL** command initiates six processes for a total of 600,000 primary electrons. The detailed **Penelope** settings in the **PROCESS** section reflect some experimentation with the parameters. The results were relatively independent of these settings.

Loading the escape file into **GenDist**, we find that it contains 610,192 electrons and 2167 photons. The extra electrons are secondaries. We set a filter in **GenDist** to limit plots and analyses to electrons with  $z > 98.0$   $\mu$ m and  $T_e > 2.0$  MeV. Figure 9 shows a plot of the angular distribution, the relative number of electrons in angular bins of width  $0.9^\circ$ . For 600,000 electrons, we expect that statistical variations between bins are on the order of 1.3%.

---

<sup>1</sup>M.Vilches, *et.al.*, *Monte Carlo simulation of the electron transport through thin slabs: A comparative study of penelope, geant3, geant4, egsrc and mcnp*, Nucl. Instrum. and Methods **254** (2007), 219.

Table 6: **GamBet** script ALUMSCAT2D.GIN

```

GEOMETRY
  DUnit = 1.0000E+06
  GFile2D = AlumScat2D.MOU (Cylin)
END
COMPOSITION
  Material = 13
  Region(1) = 1
END
SOURCE
  SList
    E 2.25E6 0.001 0.001 0.001 0.00 0.00 1.00
  End
  NPMult = 100000
END
PROCESS
  EMax = 2.5000E+06
  EAbs(Electron) = 5.0000E+04
  EAbs(Photon) = 5.0000E+04
  EAbs(Positron) = 5.0000E+04
  C1: 0.05
  C2: 0.05
  WCC: 1.0E4
  WCR: 1.0E4
  DsMax = 5.0000E+00
  StepMax = 500000
  Time = 86400
  Parallel 6
END
ENDFILE

```

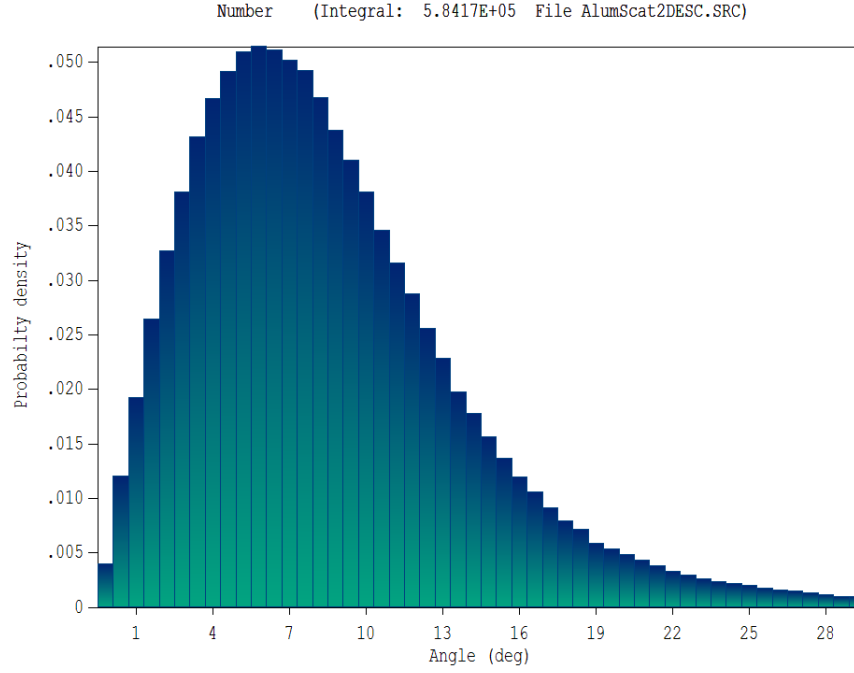


Figure 9: Histogram of the number of emerging electrons sorted by angle in  $0.9^\circ$  bins.

For a comparison to experimental results, we must divide the relative number of electrons in a bin by the solid angle of the bin. We can perform the operation automatically in **GenDist** using the `Plot data to file` command. In response, the program regenerates the plot and makes the following entry in the data file:

```
Filter status
  XMin: -1.0000E+37   XMax:  1.0000E+37
  YMin: -1.0000E+37   YMax:  1.0000E+37
  ZMin:  9.8000E+01   ZMax:  1.0000E+37
  RMin: -1.0000E+37   RMax:  1.0000E+37
  UxMin: -1.0000E+00  UxMax:  1.0000E+00
  UyMin: -1.0000E+00  UyMax:  1.0000E+00
  UzMin: -1.0000E+00  UzMax:  1.0000E+00
  TMin:  2.0000E+06   TMax:  1.0000E+37
```

Bin	AngMin (deg)	AngMax (deg)	p(Ang)	P(Ang)	dP(Ang)/DAng
=====					
1	0.0000E+00	9.0000E-01	8.9933E-03	8.9933E-03	3.5341E-03
2	9.0000E-01	1.8000E+00	2.5969E-02	3.4962E-02	3.4017E-03
3	1.8000E+00	2.7000E+00	4.1450E-02	7.6413E-02	3.2578E-03
4	2.7000E+00	3.6000E+00	5.4950E-02	1.3136E-01	3.0849E-03
5	3.6000E+00	4.5000E+00	6.5575E-02	1.9694E-01	2.8633E-03
6	4.5000E+00	5.4000E+00	7.2153E-02	2.6909E-01	2.5777E-03
...					

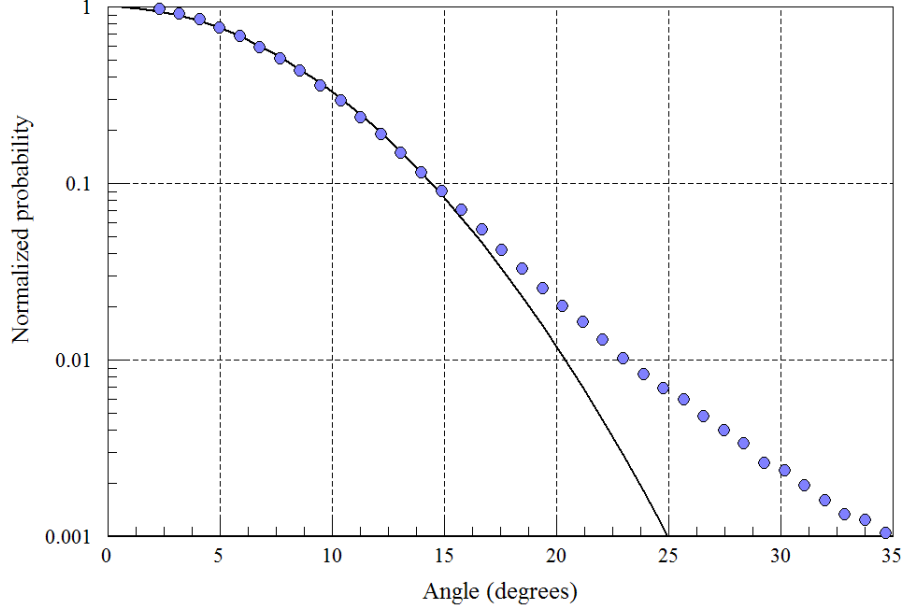


Figure 10: Angular distribution  $p(\theta)$ . The solid line is a plot of the curve of Eq. 1 with  $\theta_e = 9.5^\circ$ . The data points were derived from the **GamBet** results with a normalization factor for the best fit.

A record of the filter status is followed by bin statistics for the current plot. The final column gives the relative intensity per unit of solid angle. We want to create a plot of probability density versus the average angles of the bins. Assuming that the average angle divides the solid angle of a bin in half, it is defined by:

$$\bar{\theta} = \sqrt{\frac{\theta_{min}^2 + \theta_{max}^2}{2}}. \quad (2)$$

Figure 10 shows a normalized plot of  $p(\theta)$  (blue points) determined from **GamBet** and a plot of Eq. 1 with  $\theta_e = 9.5^\circ$ . There is very good agreement over the range  $0.0^\circ \leq \theta \leq 14^\circ$ . At higher angle, the small-angle model used to derive Eq. 1 is not valid. To get a quantitative measurement of the small-angle agreement, we can calculate the effective scattering angle implied by the data. If we assume that the simulation results follow the variation of Eq. 1, then the mean scattering angle is related to the probabilities at any two points by:

$$\theta_e = \sqrt{\frac{\theta_2^2 - \theta_1^2}{\ln[p(\theta_1)] - \ln[p(\theta_2)]}}. \quad (3)$$

Analyses of several point pairs over the valid range implies that  $\theta_e \cong 9.31^\circ$ . For comparison, the Geant results in the Vilches paper were  $7.47^\circ$  (Version 4.1),  $9.17^\circ$  (Version 6.0) and  $9.33^\circ$  (Version 8.0).

---

## 5 Electron beam energy deposition in a high-pressure gas

This example treats energy deposition in a high pressure gas by a pulsed electron beam, a situation that might be encountered in an ionization chamber. The system geometry is relatively simple to allow comparisons with theory. The example emphasizes the following features:

1. Interpretation of deposited dose for a pulsed beam in a 2D cylindrical geometry.
2. Modification of electron dynamics by an applied electric field.
3. Definition of a special material not included in the standard Penelope set.
4. Comparison of **GamBet** results to theory.

The incident electron beam with 0.5 cm radius, 1.0 A current, 125 keV kinetic energy and 1.0 ms pulselength enters a chamber of radius 5.0 cm and length 10.0 cm filled with 10 atmospheres of helium gas. We shall compare results with and without an applied accelerating field of  $E_z = -20.0$  kV/cm. In comparison, the NIST EStar site gives an electron stopping power in helium at 10 atmospheres of  $dE/dx = 6.192$  keV/cm. Therefore, the accelerating field counteracts the affect of collisional energy loss and we expect that the majority of electrons exit through the downstream boundary.

You can perform the complete calculation if you have the **TriComp Mesh** and **EStat** programs. Otherwise, we have supplied the electric field file **IONCHAMBER2D.EOU** so you can carry out the **GamBet** simulation. The input file **IONCHAMBER2D.MIN** (listed in Table 7) defines the mesh for the **EStat** calculation. The same mesh is used as the geometry file of the **GamBet** calculation. The first region is a cylinder that will be associated with the helium fill gas. This region is surrounded by void – the calculation does not include the effects of the chamber walls. The element size is about 0.1 cm. The two other unfilled regions (node assignment only) define fixed potentials on the left and right boundaries to create the electric field in the **EStat** calculation. These regions play no part in the **GamBet** simulation. Table 8 shows the contents of **IONCHAMBER2D.EIN**, the control script for the **EStat** calculation. The commands specify that units are in centimeters, cylindrical weighting should be applied, and that the helium gas has a relative dielectric constant close to unity. The potential on the entrance boundary is set to  $\phi = 0.0$  V and the right-hand boundary to  $\phi = 2.0 \times 10^5$  V. Run **Mesh** to generate the file **IONCHAMBER2D.MOU**. Optionally, run **EStat** to create **IONCHAMBER2D.EOU**.

There are two files required for the **GamBet** calculation are **IONCHAMBERINPUT2D.SRC** and **IONCHAMBER2D.GIN**. The **Circular beam tool** of the **Trak** code was used to create a PRT file that was converted to the **GamBet SRC** format. The beam consists of 100 model electrons uniformly distributed in radius to  $r = 0.5$  cm. The current of each particle is proportional to  $r$ , giving uniform current density. The sum of particle currents equals 1.0 A. Table 9 shows the contents of the file **IONCHAMBER.GIN**. The script has some interesting features:



Table 7: Script to define a mesh for the **EStat** and **GamBet** calculations

```
* File: IONCHAMBER.MIN
GLOBAL
  XMESH
    0.00  10.00  0.10
  END
  YMESH
    0.00   5.00  0.10
  END
END
REGION  FILL Helium
  L   0.00  0.00 10.00  0.00
  L  10.00  0.00 10.00  5.00
  L  10.00  5.00  0.00  5.00
  L   0.00  5.00  0.00  0.00
END
REGION  LeftBound
  L   0.00  0.00  0.00  5.00
END
REGION  RightBound
  L  10.00  0.00 10.00  5.00
END
ENDFILE
```

Table 8: Control script for the **EStat** calculation

```
* File: IONCHAMBER2D.EIN
DUnit = 100.0
Geometry = Cylin
Epsi(1) = 1.0
Potential(2) = 0.0
Potential(3) = 200.0E3
ENDFILE
```

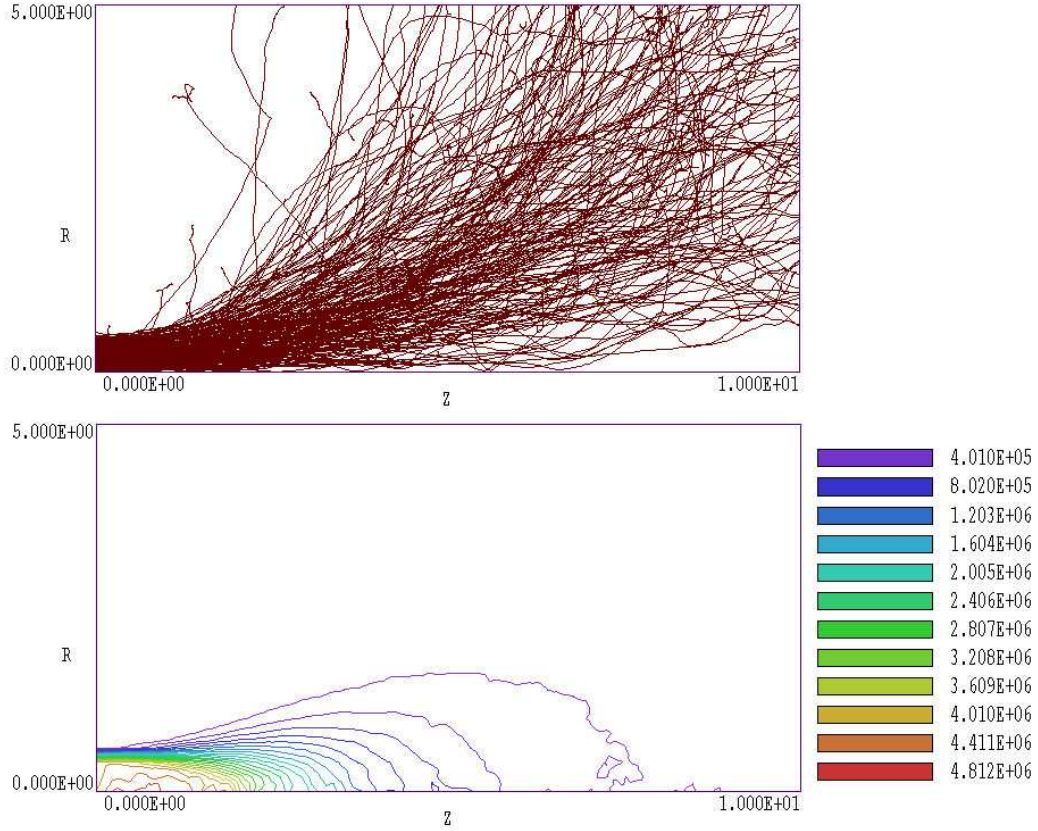


Figure 11: Results with no applied axial electric field. Top: Selected electron trajectories. Bottom: Dose distribution contours, units of Gy

- The `EFile2D` command is used to include effects of applied electric field. For a zero-field run, the command can be deactivated by placing an asterisk (the comment symbol) in the first column.
- The standard Penelope model for helium corresponds to atmospheric pressure. The `Material` structure is used to represent the high-pressure gas with density 10 times the value at STP.
- The `TPulse` command signals that **GamBet** should record dose rather than dose rate.
- The command `PlotOn 2` causes the program to record two showers for each primary particle (giving a total of 200 orbit traces).
- Note that there are no material properties defined for Regions 2 and 3 which consist of nodes only. The region numbers are not assigned to elements, and therefore the regions do not play a part in the **GamBet** calculation.

Energy statistics were recorded in the file `IONCHAMBER.GLS`. The total input energy was 125.0 J. With no applied electric field, energy was conserved to within 0.26%. The beam deposited 91.98 joules in the gas, while electrons carrying 33.02 J escape through the boundaries. With the applied field, the energy difference was 158.21%. The figure was not close to zero because the

Table 9: Control script for the GamBet calculation

```
* File: IONCHAMBER.GIN
GEOMETRY
  DUnit 100.0
  GFile2D Ion_Chamber.MOU Cylin
  EFile2D Ion_Chamber.EOU
END
COMPOSITION
  Material
    Name Helium_10atm
    Component He 1.0
    Density 1.785E-3
    Insulator
  End
  Region(1) = 1
END
SOURCE
  SFile IonChamberInput
  NPMult = 500
  TPulse = 1.0E-3
END
PROCESS
  EAbs Electron 1000.0
  EAbs Photon 1000.0
  EAbs Positron 1000.0
  C1 0.10
  C2 0.10
  WCc 5000.0
  WCr 5000.0
  EMax 300.0E3
  DsMax(1) = 0.20
  StepMax = 5000
  PlotOn 2
END
ENDFILE
```

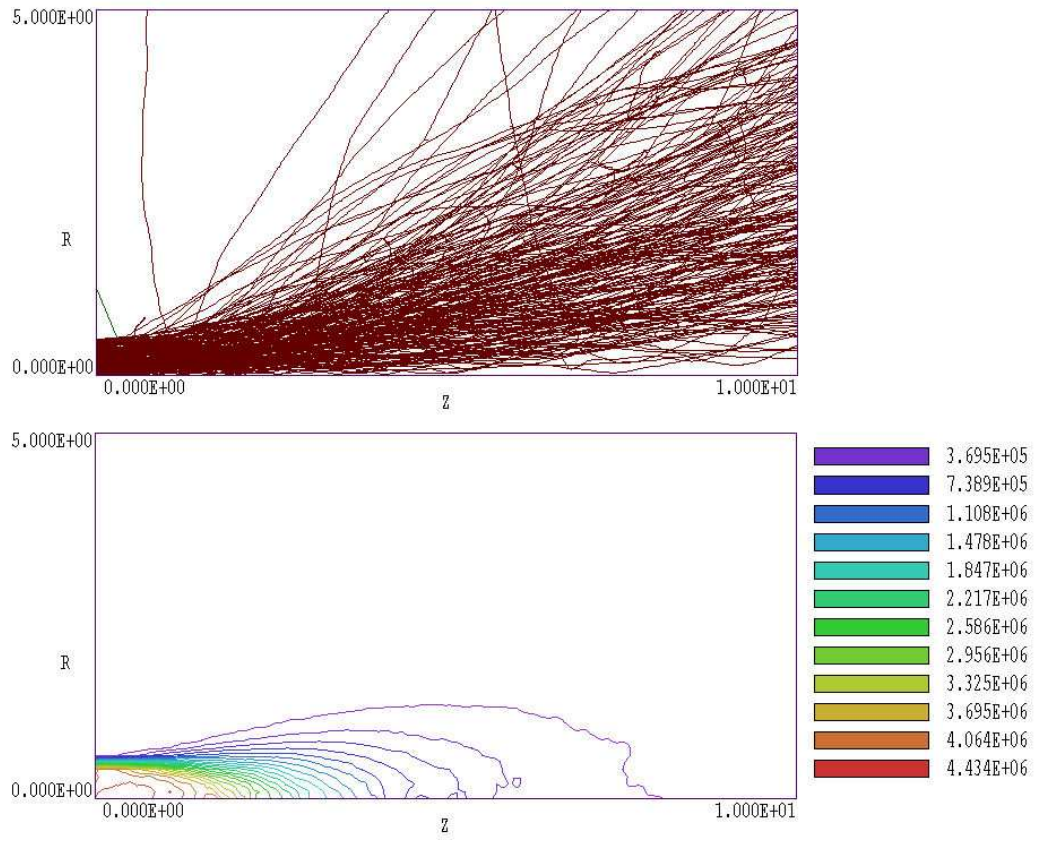


Figure 12: Results with an applied field  $E_z = 20$  kV/cm. Top: Selected electron trajectories. Bottom: Dose distribution contours, units of Gy

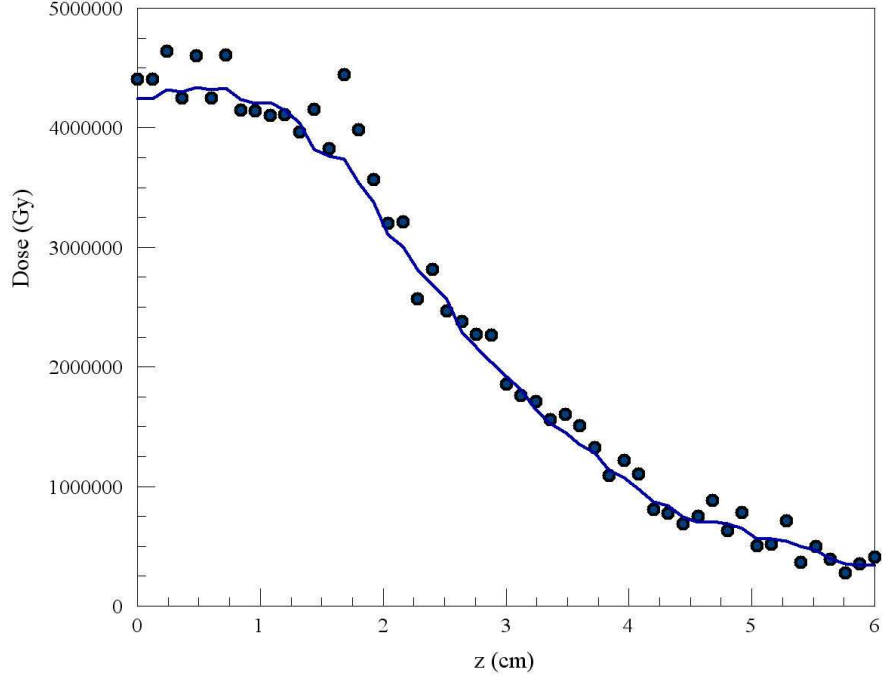


Figure 13: Variation of deposited dose along the axis. The system entrance is at  $z = 0.0$  cm. Circles: raw data. Line: data after one smoothing operation with 10 cycles.

electric field accelerated electrons within the solution volume. In this case the energy deposited in the gas dropped to 53.29 J while the energy of escape electrons increased to 269.56 J. The *Energy difference* parameter equals the difference between final and initial energies divided by the initial energy. Note that

$$(269.56 + 53.29 - 125.00)/125.00 = 1.5828.$$

Figure 11 shows selected electron trajectories and raw dose distributions for a run with no applied field. Given the EStar stopping power, we can calculate thin target dose at the entrance. The predicted energy loss per cm for a 1.0 A beam is 6.192 J, while the mass of helium in a cylinder of length 1.0 cm and cross-section area  $0.785 \text{ cm}^2$  is  $1.401 \times 10^{-6} \text{ kg}$ . The expected dose is therefore  $4.42 \times 10^6 \text{ J/kg}$ . For comparison, the entrance value in the simulation is about  $4.85 \times 10^6 \text{ Gy}$ . The higher value results from the contribution of backscattered electrons. For comparison, Fig. 12 shows orbits and dose distribution with the applied field. The orbits appear smoother because of component of directed velocity in the  $+z$  direction. The volume of significant dose extends a longer distance in  $z$  and the entrance dose is closer to the theoretical prediction because of the reduction of backscattered electrons.

Finally, Fig. 13 shows the variation of dose along the axis with distance into the gas. The plot was created by employing the line scan feature of **GBView2**, recording the results in a history file and then transferring values to PsiPlot. The circles represent values calculated directly from raw data. The level of element-to-element statistical variation is apparent. The solid line shows a scan through a smoothed distribution (10 smoothing cycles).

---

## 6 X-ray generation by a pinched electron-beam diode

The calculations described in this tutorial demonstrate the full power of **GamBet** for 2D simulations. The program uses input from the **Trak** electron gun code to characterize an X-ray source for pulsed radiography. An electron beam is generated in a pinched-beam diode. Here, the term *diode* refers to a high-voltage vacuum gap that carries a large current of electrons and ions and the term *pinched-beam* implies that the electron motion is dominated by the magnetic field generated by the current. You can perform the complete simulation if you have the **Trak** package. Otherwise, we have included **Trak** output files so you can carry out the **GamBet** calculations. The files PINCHDIODE.MIN, PINCHDIODE.EIN and PINCHDIODE.TIN are inputs for **Trak**. The code produces two output files: PINCHDIODEP.EOU (data on the self-consistent electric and toroidal magnetic fields in the diode region) and PINCHDIODE.PRT (final parameters of model electrons and ions). The file PINCHDIODEE.PRT is a filtered version that contains only electrons that strike the target. The file PINCHDIODEX.MIN defines the geometry mesh for the **GamBet** simulation and PINCHDIODEX.GIN controls the run.

Figure 14 shows the diode geometry. The tungsten rod anode has a diameter of 1 mm, while the thin aluminum tube cathode has an inside diameter of 10.0 mm. The anode protrudes 4.0 mm into the cathode cavity. An applied pulsed voltage of 1.2 MV creates plasmas on the cathode and anode surfaces which act as sources for an intense flow of ions and electrons. The magnetic field generated by the current pushes electrons to a small spot on the anode tip. In the **Trak** simulation, electrons are emitted at the space-charge limit over the full exposed surface of the cathode. We assume that ion emission occurs over a 4.0 mm length near the anode tip – the ion flux illuminates most emitting regions on the cathode. Run the **Mesh** program to process and to save the electric-field mesh (PINCHDIODE.MOU) and run **EStat** to create an applied electric-field solution (PINCHDIODE.EOU). Next run **Trak** with PINCHDIODE.TIN as input. You can use **Trak** to inspect particle orbits in the self-consistent electric and magnetic fields. The top part of Fig. 14 shows selected electron orbits and lines of constant electrostatic potential while the bottom part plots selected ion orbits and contours of  $B_\theta$ . Note the smooth compression of electron flow by the toroidal magnetic field with stagnation at the anode tip. Figure 15 shows that about 75% of the electron current (18.44 kA) is deposited within 1.0 mm of the anode tip.

The file PINCHDIODE.PRT created by **Trak** contains the final parameters of all particles, including ions and electrons that stagnate near the cathode. For the **GamBet** run, the distribution must be filtered to include only electrons that strike the target. In **GenDist**, load the file with the **File (PRT/SRC)/Load PRT file** command. Set up a filter that passes only electrons by setting the maximum mass to 0.9 AMU. Set the maximum kinetic energy to 1.0 MeV to admit only electrons that reach the anode. Save the filtered distribution as PINCHDIODEE.PRT.

The next step is to create a geometry file for **GamBet**. We use a simplified version of the geometry of Fig. 14 that contains only features relevant to the Monte Carlo calculation. Run **Mesh** with PINCHDIODEX.MIN to create PINCHDIODEX.MOU. Figure 16 shows the geometry mesh. It contains a portion of the tungsten anode surrounded by a spherical void of radius 15.0 mm centered at the anode tip. The thin aluminum cathode has been omitted because it has a negligible effect on photon transport. The void region is large enough to track the orbits of backscattered electrons emerging from the target. In the field-free tungsten region

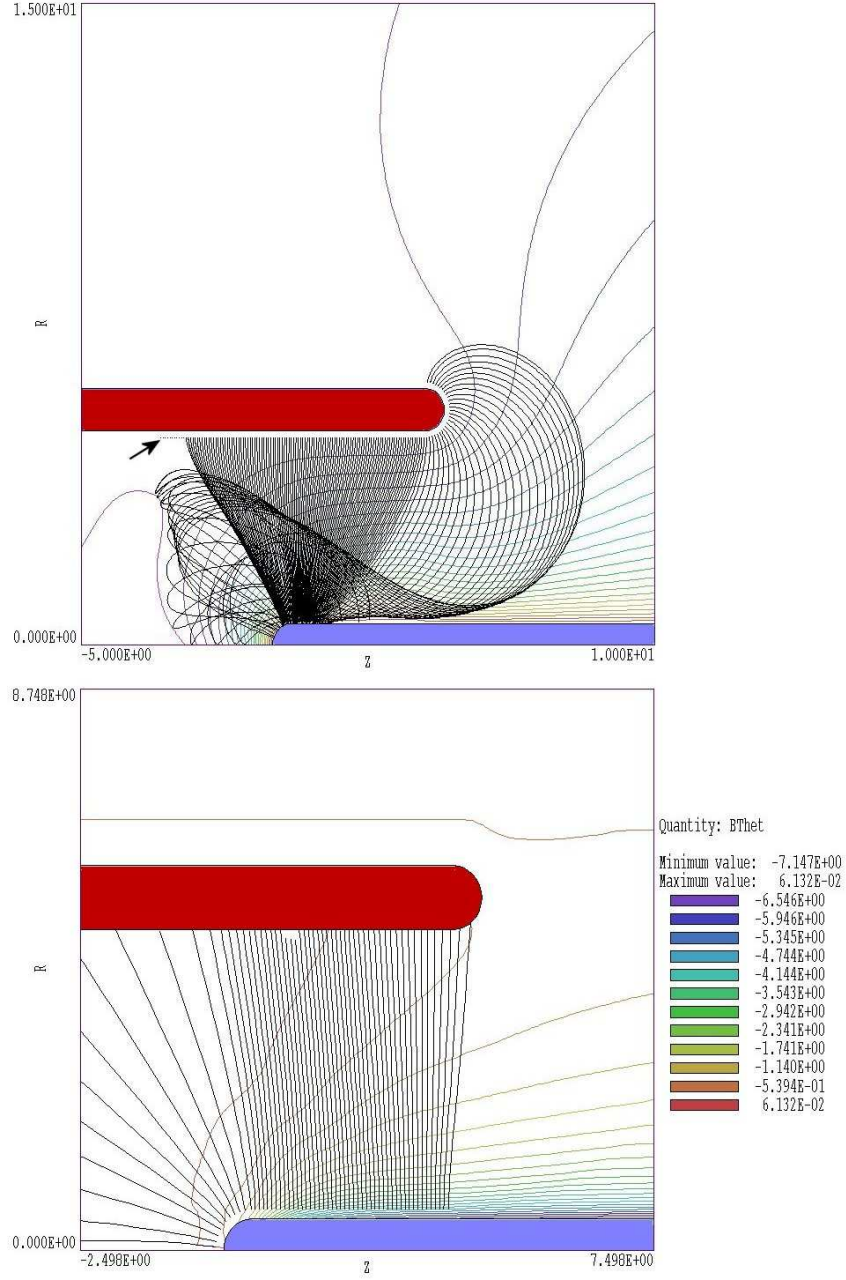


Figure 14: Nested-cylinder diode, 1.2 MV, dimensions in mm. Top: selected electron orbits and lines of constant electrostatic potential. Bottom: Lines of constant  $B_\theta$  and selected ion orbits.



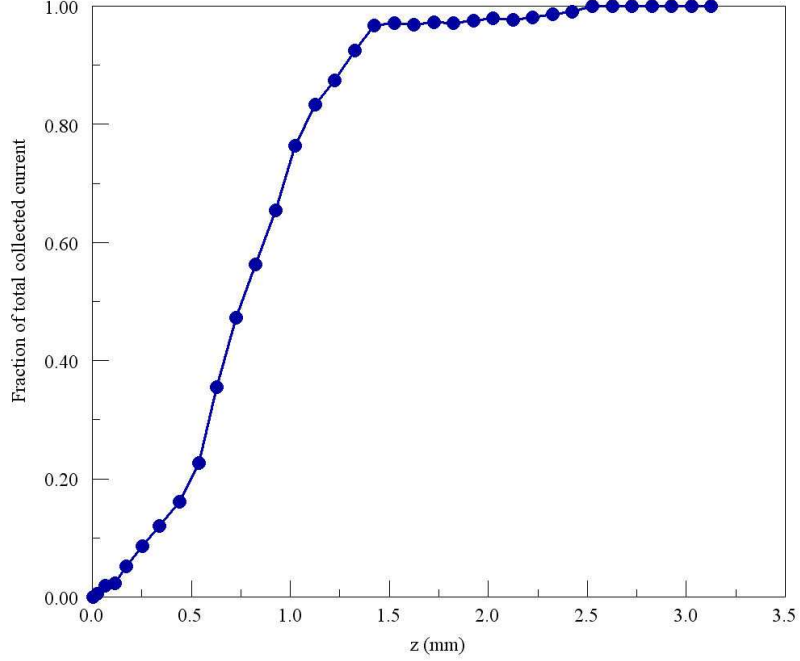


Figure 15: Total electron current collected on the target as a function of distance from the tip

electrons interact with the material producing bremsstrahlung photons. There are no material interactions in the void region. Here, backscattered electrons are reflected by the radial electric field and drift away from the tip under the influence of the toroidal magnetic field. Photons travel through the void unimpeded to the boundary where their properties are recorded in the escape file. Note that **GamBet** stops photon orbits exactly at the boundary, even through the mean-free path from the last interaction may be substantially larger than the void radius. Precise termination at the spherical boundary makes it possible to back-project the orbits to determine the effective spot size of the X-ray source.

Table 6 shows the contents of the **GamBet** script PINCHDIODEX.GIN. In response to the **GFile2D** command, the program loads the geometry mesh of Fig.16 and applies cylindrical weighting. The **EFile2D** command loads the electric field file created with the **Trak EDump** command. The *RelMode* calculation includes data for the toroidal magnetic field. The **SFile** command loads the electron source file derived from the **Trak** particle file output. **GamBet** generates 50 showers for each incident particle. To speed the calculation, electrons and photons below a cutoff value of 50 keV are absorbed *in situ*. Lower energy photons would be absorbed in the vacuum chamber walls surrounding the diode and would not contribute to the available dose. A bremsstrahlung forcing factor of 200 is used to improve statistics.

Figure 17 shows contours of electron energy deposition in the tungsten anode. The plot emphasizes the unique capability of **GamBet** to score interactions using elements as sub-zones. The energy-deposition profile is consistent with Fig. 15. The plot also shows drift orbits of backscattered electrons, which move away from the tip in the combined electric and magnetic fields. Figure 18 shows the angular distribution of photons in the escape file. The top (direct output from **GenDist**) shows the distribution as a function of polar angle relative to the  $z$  axis of the diode. The bottom graph plots a derived quantity, the relative flux per unit solid angle. The photon flux is almost uniform over most of the sphere. It drops to zero at  $0^\circ$  and  $180^\circ$

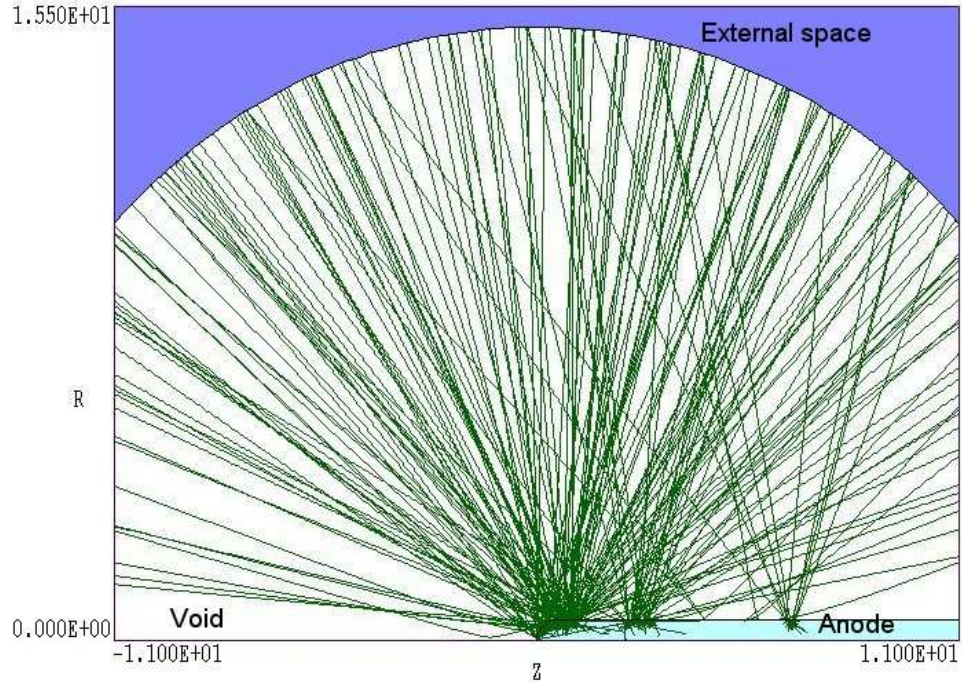


Figure 16: View of a section of the GFile geometry for the **GamBet** simulation showing selected photon trajectories

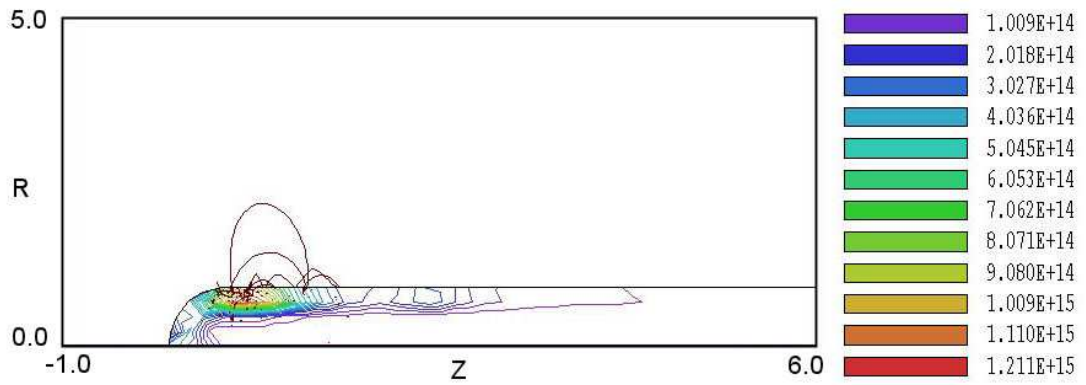


Figure 17: Dose-rate deposition profile in the target in units of Gy/s.

Table 10: **GamBet** control script PINCHDIODEX.GIN

```

* Regions
*      1      VOID
*      2      TARGET
GEOMETRY
  DUnit 1000.0
  GFile2D PINCHDIODEX.MOU Cylin
  EFile2D PINCHDIODEP.EOU BTheta
END
COMPOSITION
  Material W
  Region(1) = Void
  Region(2) = 1
END
SOURCE
  SFile PINCHDIODEE
  NPMult = 50
END
PROCESS
  EAbs Electron 5.0E4
  EAbs Photon 5.0E4
  EAbs Positron 5.0E4
  C1 0.20
  C2 0.20
  WCc 10000.0
  WCr 10000.0
  EMax 1.4E6
  DsMax(1) = 0.02
  DsMax(2) = 0.05
  StepMax = 20000
  PlotOn 200
  Force Brems 200.0
END
ENDFILE

```

because of absorption in the rod target. The general decrease at small forward angles reflects the angular distribution of electrons striking the tip.

The **Analysis/Transform distribution** command of **GenDist** was used to reverse the photon distribution recorded in the file **PINCHDIODE.SRC**. In this case the distribution was filtered to include only photons exiting at the radius of the spherical void. The photon positions were moved back a distance 15.0 mm to determine the approximate positions of origin. The data were saved in a new **SRC** file and used in **GenDist** to create the plot of Fig. 18. The figure shows that the effective source size is less than 1 mm in the axial direction. We can also use the escape file to determine the radiation conversion efficiency. The statistics window displayed when **PINCHDIODE.SRC** is loaded shows that the file contains 618,836 photons with an average energy of 237.3 keV. The file **PINCHDOPDEE.PRT** contains 429 electrons with average energy equal to 1.17 MeV. We must also factor in the effects of the bremsstrahlung forcing factor of 200 and the multiplication factor of 40. The photon conversion efficiency is therefore:

$$\frac{618836 \times 0.2373}{200 \times 40} \frac{1}{429 \times 1.17} = 3.7\%.$$

The ideal conversion efficiency with no target absorption listed on the NIST EStar site is 6.7%.

Another quantity of interest is the radiation dose produced at points removed from the diode. We could use information in the escape file to make an analytic estimate, but the calculation is quite complex. It is easier to apply **GamBet** directly. To perform the calculation, we create an alternate solution geometry with an aluminum shell outside the void as shown in Fig. 20 and determine the average dose in the shell. The figure is then adjusted for the beam pulselength and extrapolated to the desired radius. The input files for the calculation are **PINCHDIODED.MIN** and **PINCHDIODED.GIN**. The **GamBet** run generates the dose file **PINCHDIODED.G2D** which is loaded into **GBView2**. Figure 20 shows an element plot of the dose rate from energy deposition by secondary electrons generated by the photons. The data is statistically noisy, so we use the **Dose analysis/Region properties** command to calculate an area-weighted average over the aluminum shell. The results (shown in the box at the bottom of the figure) are  $7.848 \times 10^8$  Gy/s for secondary electron processes and  $2.270 \times 10^8$  Gy/s for direct photon processes. The total dose rate is  $1.012 \times 10^9$  Gy/s. If we had a 15 ns beam pulse, the dose at a distance of 100 cm would be

$$(1.012 \times 10^9) (15.0 \times 10^{-9}) (1.55/100)^2 = 3.416 \times 10^{-3} \text{ Gy}$$

or 314.6 mrad.

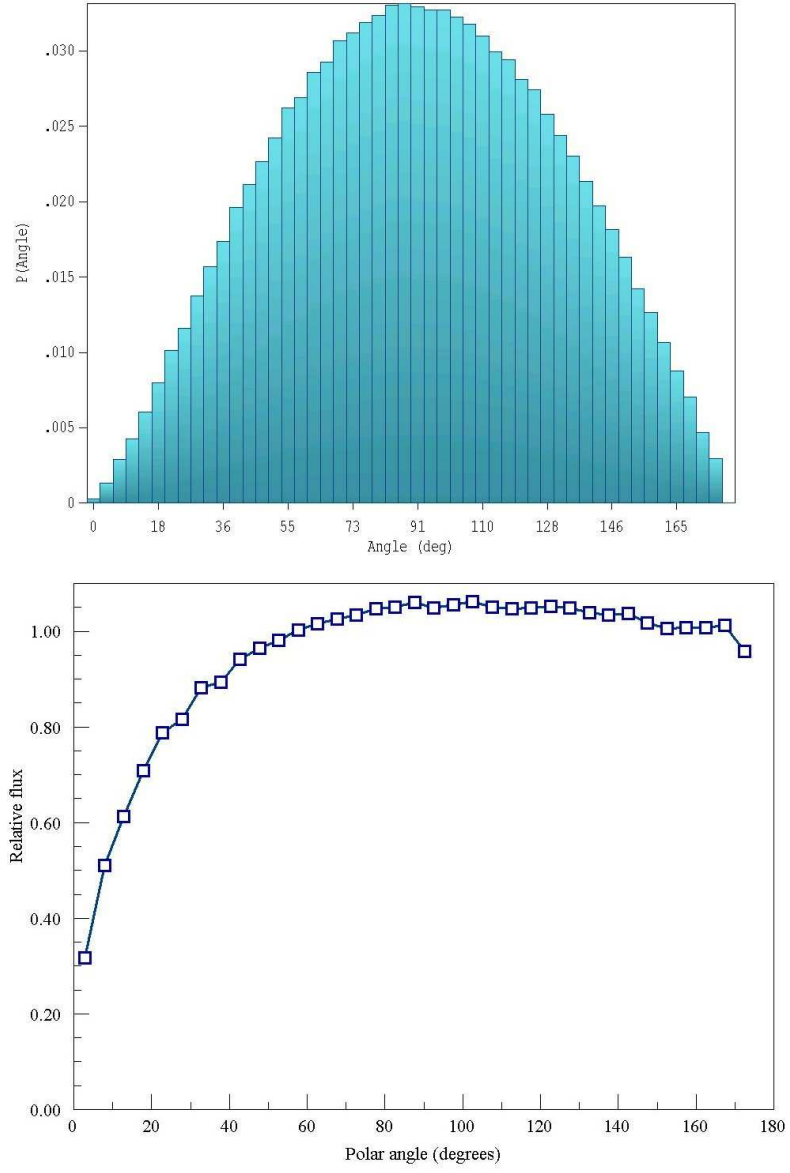


Figure 18: Relative fraction of escape photons (top) and flux per unit solid angle (bottom) as a function of polar angle.

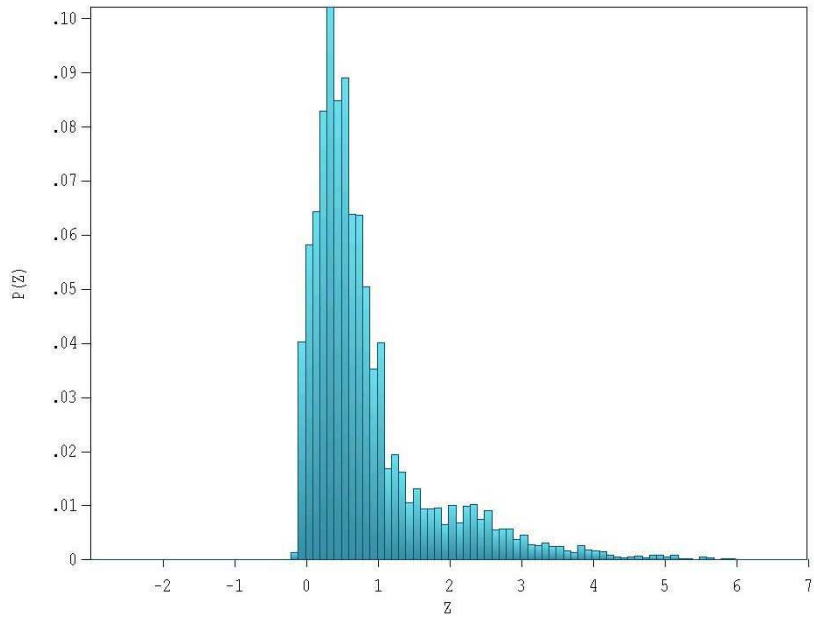


Figure 19: X-ray source size – axial distribution of photon starting positions

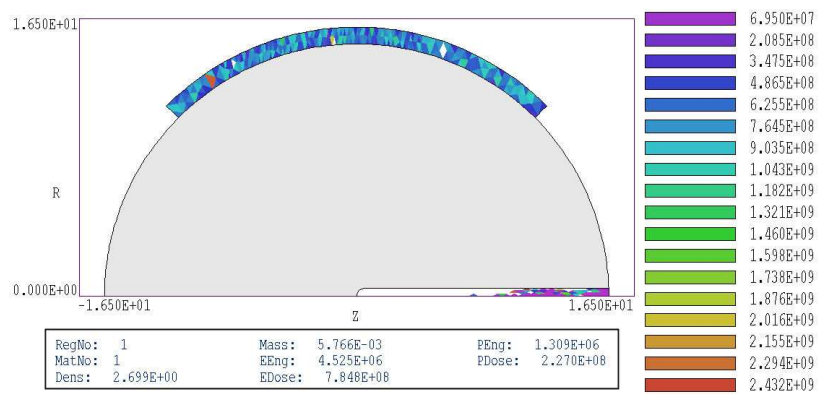


Figure 20: Alternate geometry for calculating available dose from the source. Element plot with adjusted limits shows the dose rate in the aluminum shell. The results of a region calculation is shown in the box at the bottom.



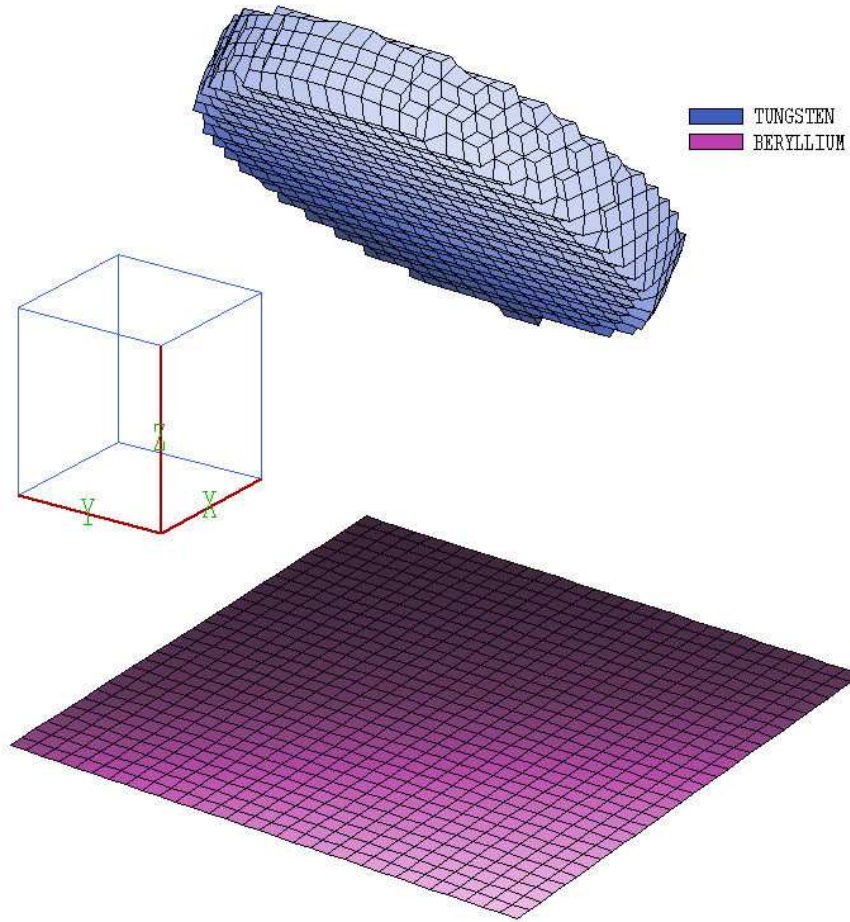


Figure 21: Three-dimensional view of the system geometry defined by `XRAYTARGET.MIN`

## 7 X-ray generation from an inclined target

The example discussed in this section addresses a three-dimensional simulation. A beam of 100 keV electrons is incident on a tungsten target inclined at  $45^\circ$ . The resulting bremsstrahlung electrons are transversely extracted through a thin beryllium foil. The tutorial has three goals:

1. Demonstrate the setup techniques for three-dimensional calculations.
2. Calculate the energy efficiency for the generation of extracted X-rays including the effects of absorption in the target and vacuum window.
3. Compare the photon energy spectrum to experimental results.

The run requires three input files: `XRAYTARGET.MIN`, `XRAYTARGET.GIN` and `XRAYTARGET.PRT`. The first file defines the system geometry, the second controls the **GamBet** run, and the third gives the parameters of the incident electron beam.



Figure 21 shows the geometry created by the **MetaMesh** commands listed in Table 11. The incident beam moves in the  $+x$  direction at position  $y = 0.0''$ ,  $z = 0.625''$ . The tungsten target with a radius of  $0.30''$  and thickness  $0.10''$  is inclined at an angle of  $45^\circ$  with respect to the beam and the exit window. The solution volume has widths  $0.75''$  along  $x$  and  $y$ . A beryllium window at  $z = 0.0''$  extends over the lower surface of the solution volume. The system is composed of three objects: 1) the solution volume (a box that has *Void* properties in **Gambet**), 2) the tungsten target and 3) the beryllium window of thickness  $0.002''$ . **MetaMesh** can represent almost any geometry, but good choices reduce the work and the possibility of errors:

- In initial solutions, keep the geometry simple by including only essential objects. Later, you can add additional structures like collimators.
- Because the beryllium window lies in a plane normal to an axis, it would be easy to model the thin structure directly. On the other hand, if the foil were rotated or had a non-planar shape, a large number of very small elements would be required to resolve it. This solution demonstrates one technique to avoid tiny elements. In **MetaMesh** we increase the thickness of the foil by factor of 10 and in **Gambet** we use a material density  $1/10$  of the solid value. The modified foil is thin compared to the simulation scale size and has almost the same effect on particles.
- Conformal fitting is applied on the critical front face of the target. Edge fitting is not employed, accounting for the irregular elements on the rim (Fig. 21). A perfect fit on the edges would require significant element distortions but would not contribute to the physical results.
- The element sizes used in the *ZMesh* structure ensure that the foil has the correct surface without fitting operations. The work required in **MetaMesh** can often be reduced with some forethought.

The incident electron beam file `XRAYTARGET.PRT` was generated using the *Circular beam tool* in **OmniTrak**. With this resource a large distribution can be generated by supplying a few parameters in the dialog of Fig. 22. The tool automatically creates beams in 3D space with particles transversely distributed in a hexagonal pattern. The settings in Fig. 22 call for an electron beam with 100 keV kinetic energy moving in the  $+x$  direction. The beam has a radius of  $0.080''$  with an average position  $y = 0.0''$ ,  $z = 0.625''$  in the plane at  $x = -0.1''$ . Any starting  $x$  position is suitable as long as all electrons start outside the target. The file defines 241 primary particles.

Table 12 shows the *Composition* section of the file `XRAYTARGET.GIN`. The section defines two materials: the standard Penelope model is used for tungsten at normal density and a special *Material* section is used for beryllium at  $1/10$  normal density. The first region of the solution volume has the *Void* property and the second and third regions are associated with materials. The assignment  $NPMult = 100$  instructs the program to generate 100 showers for each primary particle. The bremsstrahlung forcing factor of 50.0 ensures good output statistics. The command *PlotOn 2* calls for a record of primary and secondary particle trajectories for two showers for each primary particle. **Gambet** records orbits during 482 showers.

The run requires 354 seconds on a 3.4 GHz computer. Figure 23 shows particle trajectories for selected showers. The ordered set of brown lines represents the incident electron beam. The

Table 11: Contents of file XRAYTARGET.MIN – dimensions in inches

```

GLOBAL
  XMesh
    -0.375  0.375  0.025
  End
  YMesh
    -0.375  0.375  0.025
  End
  ZMesh
    0.000  0.020  0.010
    0.020  1.000  0.025
  End
  RegName(1) Void
  RegName(2) Tungsten
  RegName(3) Beryllium
END
PART
  Region Void
  Type Box
  Fab 0.75 0.75 2.00
END
PART
  Region Tungsten
  Type Cylinder
  Fab 0.300 0.100
  Rotate 0.0 45.0 0.0
  Shift 0.0 0.0 0.6957
  Surface Region Void
END
PART
  Region Beryllium
  Type Box
  Fab 0.75 0.75 0.02
  Shift 0.0 0.0 0.01
END
ENDFILE

```

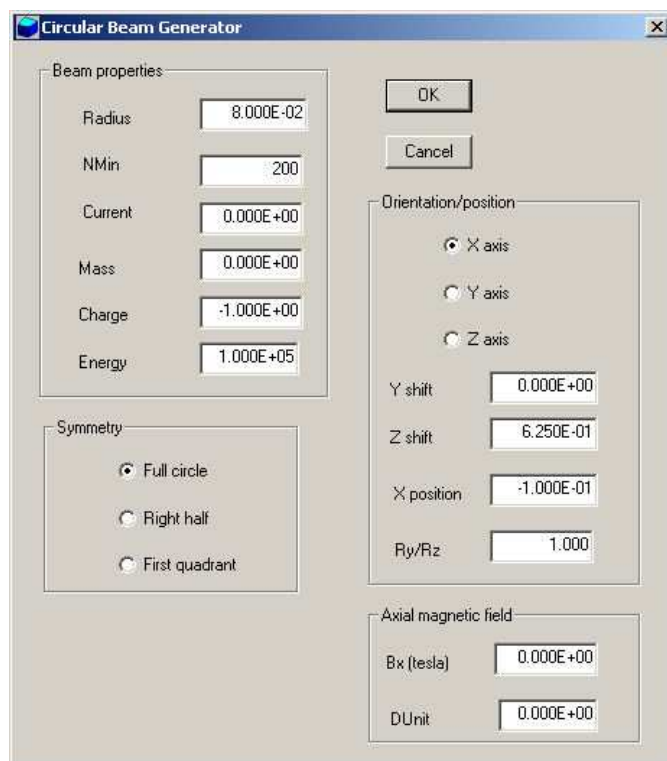


Figure 22: *Circular beam tool* dialog, **OmniTrak** program.

Table 12: Composition section of the file XRAYTARGET.GIN

```
COMPOSITION
  Material 74
  Material
    Name beryllium
    Component 4 1.0
    Density 0.1846
    Conductor
  End
  Region(1) = Void
  Region(2) = 1
  Region(3) = 2
END
```

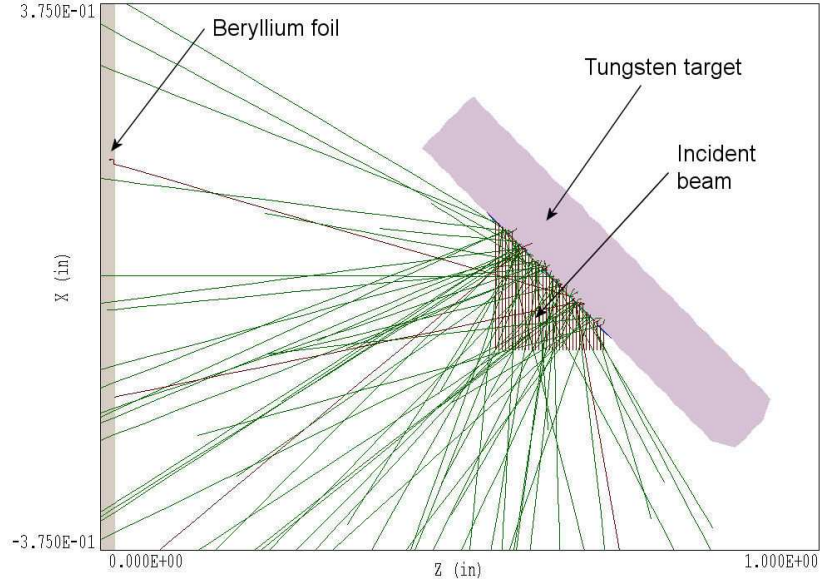


Figure 23: Slice view of the system in the plane  $y = 0.0$  showing selected particle trajectories projected to the plane. Electron orbits in brown, photon orbits in green

figure shows some backscattered electrons that strike the beryllium foil. The thickness of the tungsten target is larger than the range of photons with kinetic energy  $\leq 100$  keV. Therefore the back side is shaded with photon extraction only from the target front face. Photons and electrons travel unimpeded through the void region. The shortened lines are particles that leave the solution volume through the side faces normal to  $x$  and  $y$ .

We can use the distribution analysis functions of **GenDist** to find the efficiency of X-ray generation. We define the quantity as the energy of photons passing through the foil at  $z = 0.0$  divided by the total energy of incident electrons. To perform the analysis, load the file `XRAYTARGETESC.SRC` which contains entries for all photons and electrons that leave the solution volume. Add a filter that limits particles to photons with  $z_{max} = 0.001$ ". The filter eliminates all electrons and selected photons that exit through solution volume faces other than  $z = 0.0$ . Save the filtered distribution as `XRAYTARGETMOD.SRC` and then reload it to generate statistics. We find that the filtered file contains 729 photons with an average kinetic energy 45.69 keV. With 241 primary electrons and  $NPMult = 100$ , the input distribution consists of 24,100 electrons with kinetic energy 100.0 keV. We must include the effect of the bremsstrahlung forcing factor. The efficiency has the relatively low value:

$$\epsilon = \frac{(729)(45.69)/50.0}{(24100)(100.0)} = 2.76 \times 10^{-4} = 0.0276\%.$$

If the spatial filter is removed, the escape file contains 3411 photons with average kinetic energy 44.7 keV. The implication is that only about 22% of the available photon energy leaves through beryllium window. The net efficiency for photon generation in all directions is 0.127%. For comparison, the NIST EStar site lists the total radiation yield for 100 keV electrons in tungsten as  $Y = 1.032\%$ . The quantity is the percentage of energy lost to radiation versus small-angle collisions with electrons in the medium. Several factors contribute to the difference between the listed and the simulation values of yield. About half the created photons are directed into

the target, and a significant fraction of the remaining photons may interact before leaving the target. The listed values of  $Y$  apply to infinitely-thin targets. The average electron energy is lower in a thick target, reducing the average yield (for example,  $Y = 0.543\%$  at 50.0 keV).

To conclude, Fig. 24 illustrates bremsstrahlung X-ray spectra. The top trace (Fig. 24a) shows a measurement for a commercial X-ray tube. To generate a **GamBet** comparison, we increased the electron energy to 140.0 keV and raised the bremsstrahlung forcing factor to 200.0. The effect of the beryllium window was removed, and escape photons at all angles were included. The run generated 28,810 photons with an average kinetic energy 52.26 keV. Figure 24b shows the high-resolution spectrum created by **GamBet**. The shape closely conforms to the measured curve at high energy, clearly showing the characteristic X-rays at 59 and 66 keV. The curves differ at low energy because the experiment includes the effect of a vacuum window that attenuates long-wavelength photons.

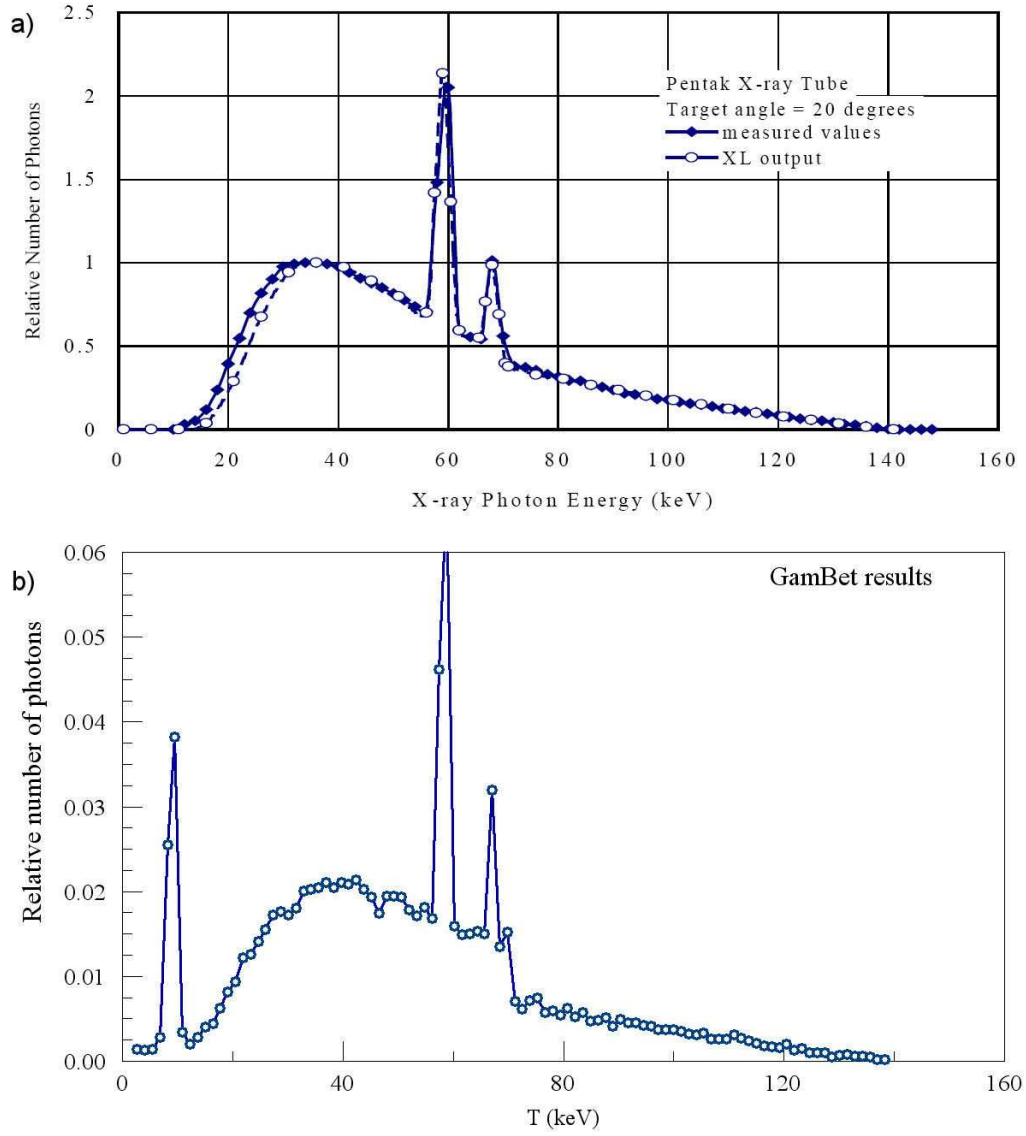


Figure 24: X-ray spectra for 140 keV electrons on a thick tungsten target. *a)* Measured values for a commercial X-ray tube. *b)* **GamBet** simulation, summation over all emission angles.

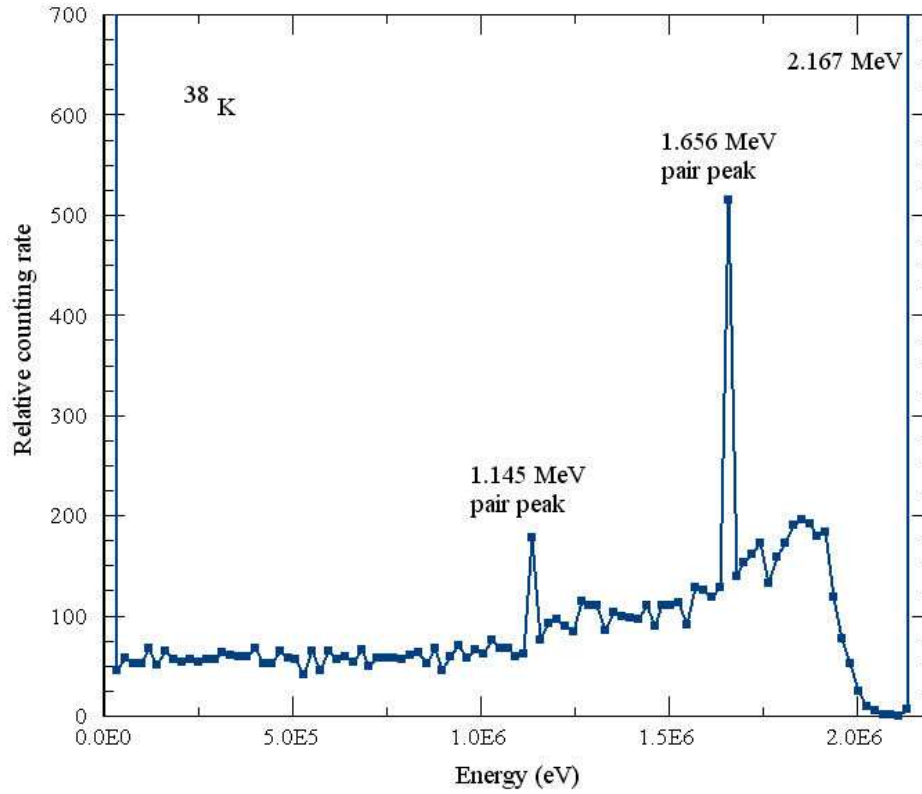


Figure 25: Pulse spectrum generated by **GamBet** for 2.167 MeV gamma rays incident on a sodium iodide detector

## 8 Pulse-height spectrum of a sodium-iodide detector

This tutorial illustrates use of the *MCA* (multi-channel analyzer) command. The feature is used to find characteristics of radiation detectors such as statistical variations in pulse amplitude or the signal spectrum of energetic particles interacting with a finite-sized device. The **NAIDETECT** example models a scintillation detector for high-energy gamma rays. There are two extreme possibilities: 1) the particle passes through the scintillator with no interaction or 2) the particle deposits all its energy in the scintillator through a series of interactions. There are a variety of possibilities in between such as a Compton scattering event followed by escape of the gamma ray. The reference G.F. Knoll, **Radiation Detection and Measurement** (Wiley, New York, 1979), Chap. 10 is a good source of information on radiation spectroscopy with scintillators.

The example files **NAIDETECT.MIN** and **NAIDETECT.GIN** describe a bare, cylindrical sodium iodide scintillator with diameter and length equal to 7.62 cm. The geometric mesh contains a single region (number 1). A  $^{38}\text{K}$  source provides gamma rays with kinetic energy  $E_0 = 2.167$ . The particles are injected on axis at the entrance face of the scintillator. Table 13 shows the complete **GamBet** control script **NAIDETECT.GIN**. There is a single primary particle with a large number of showers ( $NPMult = 20,000$ ) for good statistics. The command of interest is:

Table 13: Control script NAIDETECT.GIN

```

GEOMETRY
  DUnit 100.0
  GFile2D NAIDETECT.MOU Cylin
END
COMPOSITION
  Material 253
  Region(1) = 1
END
SOURCE
  SList
    P 2.167E6 0.0001 0.000 0.0001 0.00 0.00 1.00
  End
  NPMult = 20000
END
PROCESS
  EAbs Electron 1.0E4
  EAbs Photon 1.0E4
  EAbs Positron 1.0E4
  C1 0.10
  C2 0.10
  WCc 1000.0
  WCr -1000.0
  DsMax(1) = 0.10
  EMax 3.0E6
  MCA 100 1 2
END
ENDFILE

MCA 100 1

```

In response to the command, **GamBet** records 20,000 values of the energy deposited in region 1 in a file NAIDETECT.PLS. At the end of the run, the program uses the information to construct a histogram with the showers divided into 100 bins depending on the deposited energy.

Table 14 shows the initial lines of the file NAIDETECT.PLS. The deposited energy in the first data line (shower 1) has the value 0.0 eV. Here the photon passed through the detector with no interaction. The second data line value of 1.8599 MeV implies that the photon of shower 2 lost 86% of its energy before escape. The data can be used to determine the scintillator efficiency, defined as the probability that an incident photon deposits some of its energy. We use the sort function of a text editor to put the lines in order of increasing energy and then check the number of lines with value 0.0. There are 6481 zero-energy data lines, implying a scintillator efficiency of 68%.

Table 15 shows a portion of the histogram created by **GamBet** in the listing file NAIDETECT.GLS. The number of entries in the final bin (5054) implies that about 25% of the incident photons deposited their full energy in the scintillator. Figure 25 shows a plot created by porting the



Table 14: Initial section of file NAIDETECT.PLS

GamBet Pulse-height Distribution File (Field Precision)

RunName: NaIDetect

NLines: 20000

Regions: 1

Units: eV/p

0.0000E+00

1.8599E+06

0.0000E+00

9.7949E+05

0.0000E+00

4.9930E+05

5.2913E+05

1.7106E+06

0.0000E+00

0.0000E+00

0.0000E+00

0.0000E+00

0.0000E+00

0.0000E+00

1.2545E+06

6.9307E+05

...

histogram values to PsiPlot. There are strong peaks at  $E = 0.0$  MeV and 2.167 MeV. A continuous distribution of events corresponding to Compton scattering extends over a range of energy from 0.0 MeV to a value below the peak. Here, the resulting high-energy electron deposits its full energy in the scintillator and the reduced-energy gamma ray escapes. The value for upper energy of the Compton continuum is:

$$E = E_0 \left( \frac{1}{1 + m_e c^2 / E_0} \right) = 1.938 \text{ MeV}.$$

The lower peak within the continuum represents pair production processes where both gamma rays from annihilation of the positron escape the scintillator. In this case, the deposited energy is given by

$$E = E_0 - 2m_e c^2 = 1.145 \text{ MeV}.$$

The other pair production peak corresponds to events where only one annihilation photon escapes the medium. The deposited energy is  $E = E_0 - m_e c^2 = 1.656 \text{ MeV}$ .

For comparison, Fig. 26 shows an experimentally-measured spectrum for the same source and scintillator dimensions. Although Figs. 25 and 26 are in general agreement, the peaks in experimental trace have a significant width. Several features of the experiment account for the peak width:

- Photons are incident over the full face of the scintillator.
- The light-collection efficiency varies depending on the location of the interaction.
- There are statistical variations in the response of the photomultiplier and detection circuit.

The **GamBet** simulation includes effects of the finite scintillator size, but does not model effects of imperfections in the light-collection efficiency and detector response.

Multiple primaries may be employed to represent more complex input distributions. For example, to model uniform flux over the face of the scintillator we could use **GenDist** to create a particle distribution with radius equal to that of the scintillator distributed radially with probability function  $p(r) \sim r$ . We could also use a spreadsheet or **GenDist** to construct a set of primaries with any distribution of kinetic energy. **GamBet** processes showers using *NPMult* as the outer loop and the set of primaries as the inner loop. The values recorded in the `RunName.PLS` file equal the deposited energy integrated over the primaries per instance of *NPMult* divided by the number of primaries.

Table 15: Extracts from histogram in file NAIDTECT.GLS

Deposited energy distribution for Region 1

Energy(min):	0.0000E+00	
Energy(max):	2.1670E+06	
dEnergy:	2.1670E+04	
EDn	EUp	NEvent
(ev)	(eV)	
=====		
0.0000E+00	2.1670E+04	6541
2.1670E+04	4.3340E+04	45
4.3340E+04	6.5010E+04	58
...		
1.8420E+06	1.8636E+06	196
1.8636E+06	1.8853E+06	192
1.8853E+06	1.9070E+06	180
1.9070E+06	1.9286E+06	183
1.9286E+06	1.9503E+06	119
1.9503E+06	1.9720E+06	78
1.9720E+06	1.9936E+06	53
1.9936E+06	2.0153E+06	25
2.0153E+06	2.0370E+06	10
2.0370E+06	2.0587E+06	6
2.0587E+06	2.0803E+06	1
2.0803E+06	2.1020E+06	1
2.1020E+06	2.1237E+06	0
2.1237E+06	2.1453E+06	7
2.1453E+06	2.1670E+06	5054

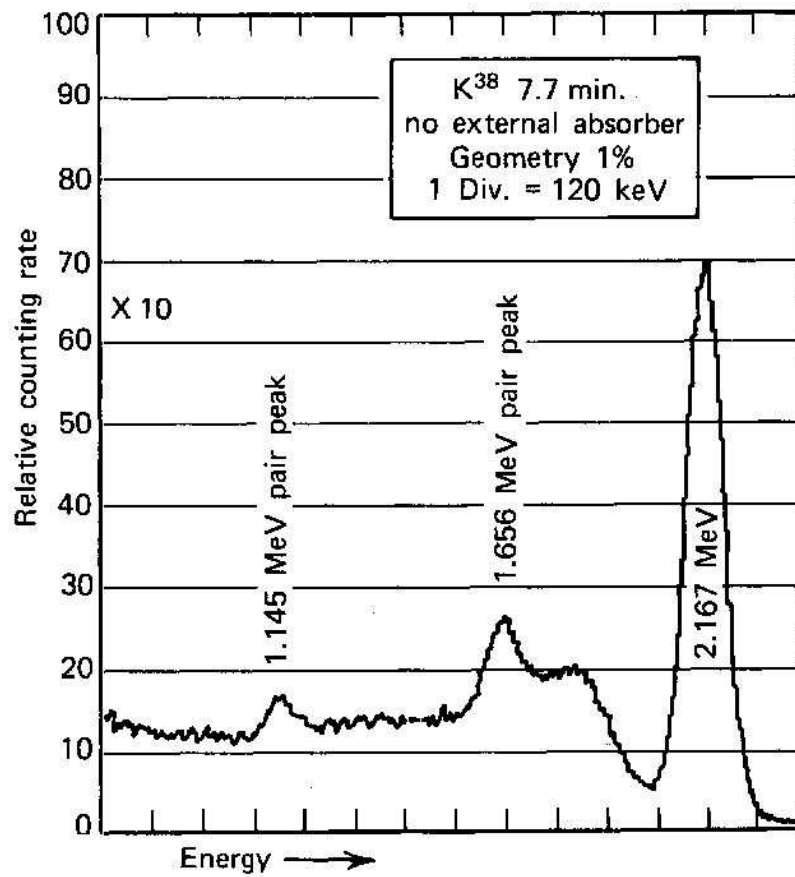


Figure 26: Measured pulse spectrum for 2.167 MeV gamma rays incident on a sodium iodide detector, from G.F. Knoll, **Radiation Detection and Measurement** (Wiley, New York, 1979), 331. (Note that the energy axis is offset.)

## 9 Beam passing through a thin foil

There are many applications where a beam of electrons passes through a thin foil (such as a vacuum window) and then traverses a vacuum region or gas to a target. Usually the foil thickness is much smaller than the scale size of the transport region. It is inefficient and inaccurate to model the processes with a single mesh with large disparities of scale. It is better to split the calculation into two stages, separating small and large scales.

This tutorial illustrates the approach with the calculation of the forward bremsstrahlung dose generated by a pulsed radiographic accelerator. The run parameters represent the DARHT I accelerator at Los Alamos National Laboratory<sup>2</sup>. The machine produces a tightly-focused electron beam with kinetic energy 19.8 MeV, current 2.0 kA and pulse length 60.0 ns. We assume the beam is incident on a tantalum target of thickness 1.5 mm. For comparison, the electron range in tantalum is 5.7 mm. A thin target is employed to limit the effective bremsstrahlung spot size set by electron diffusion. Furthermore, thicker targets do not significantly increase the forward dose because of the effects of electron scattering and target absorption. The goal of this study is to find the dose distribution in a steel phantom at a distance of 1000.0 mm from the target face. The calculations have two-dimensional cylindrical symmetry.

The first step is to find the distribution of electrons and bremsstrahlung photons from the target exit face. The **Mesh** input file `DARHT01.MIN` describes a single region that covers the range  $0.0 \text{ mm} \leq z \leq 1.5 \text{ mm}$  and  $0.0 \text{ mm} \leq r \leq 5.0 \text{ mm}$ . Table 9 lists the **GamBet** script. Commands of the **Geometry** section set cylindrical symmetry and working units of millimeters. The mesh region has the properties of tantalum. The program launches 20,000 primary electrons at a point near the axis at the front target face. The primary electrons carry a total current of 2.0 kA. A bremsstrahlung forcing factor of 25 is used for good statistics. The combined effects of the forcing factor and the value of `NpMult` give a total number of forward photons just below 1,000,000 (the limit on the number of primary particles in **GamBet**).

The run generates the escape file `DARHT01ESC.SRC` containing the parameters of particles leaving all surfaces of the solution volume. Loading the file into **GenDist**, we find the total number of photons is  $N_p = 895828$  with an average kinetic energy  $T_p = 2.698 \text{ MeV}$ . The radiation conversion efficiency (total energy of photons divided by energy of incident electrons) is given by

$$\epsilon_{rad} = \frac{N_p T_p}{N_{pmult} F_b T_e}, \quad (4)$$

where  $F_b$  is the bremsstrahlung forcing factor and  $T_e$  is the energy of the incident electrons. For this example,  $\epsilon_{rad} = 24.4\%$  compared to the tabulated maximum yield for a thick target of 43.7%. For the dose calculations we are interested only in forward-directed particles. The filter function in **GenDist** is employed to admit only particles leaving the exit target face ( $z > 1.499 \text{ mm}$ ). The filtered distribution is saved as file `DARHT_TOTAL.SRC`. The filter is then modified to include only photons (saved in `DARHT_PHOTON.SRC`). The forward current of primary and knock-on electrons is 1.749 kA with an average kinetic energy 8.828 MeV. The positron

---

<sup>2</sup>M.J. Burns, *et al.*, *Status of the DARHT Phase 2 Long-Pulse Accelerator* (**Proc. 2001 Particle Accelerator Conf.** (IEEE, 0-7803-7191-7, 2001), 325.

Table 16: **GamBet** input file DARHT01.GIN.

```

* File: DARHT01.GIN
* 19.8 MeV , 2.0 kA electron beam incident on a
* tantalum target
GEOMETRY
  GFile2D DARHT01.MOU Cylin
  DUnit 1000.0
END
COMPOSITION
  Material 73
  Region(1) = 1
END
SOURCE
  SList
    E 19.8E6 0.00001 0.00 0.00001 0.00 0.00 1.00 2.0E3
  End
  NPMult = 20000
END
PROCESS
  EAbs Electron 2.5E5
  EAbs Photon 2.5E5
  EAbs Positron 2.5E5
  C1 0.10
  C2 0.10
  WCc 2.5E5
  WCr -2.5E5
  DsMax(1) = 0.10
  Force Brems 25.0
END
ENDFILE

```

current is 16.49 A with average energy 4.331 MeV. The forward bremsstrahlung photons have an average energy 2.863 MeV. About 50% of the photons are contained within an angle of  $30^\circ$  with respect to  $z$  axis.

The two **SRC** files may be as used sources for a variety of dose calculations. To begin, consider the dose at a distance of 1 m if a sweep magnet is used to remove the electrons and positrons. The mesh defined by **DARHT02.MIN** has a drift zone of length 1000 mm and a target zone of length 100 mm. The radial width is 200 mm. The element resolution is 10.0 mm in  $r$  and in  $z$  in the drift region. A reduced axial element size of 2.5 mm is used in the target to resolve the variation of dose with depth. The **GamBet** input script **DARHT02.GIN** includes several commands of interest:

```
Material 26
Region(1) = Void
Region(2) = 1
SFile DARHT_PHOTON
NPMult = 4
TPulse: 60.0E-9
StepLimit
DsMax(1) = 100.0
DsMax(2) = 10.0
NoEscape
```

The drift region is treated as a *Void* because air at atmospheric pressure would have little effect on the photons. The file **DARHT\_PHOTON.SRC** contains only forward-directed photons. The choice  $NpMult = 4$  gives sufficiently small statistical variations. The command  $TPulse = 60.0$  ns signals that output quantities should be recorded in units of Gy rather than as dose rates. As in any photon computation with multiple regions, it is prudent to set values of **DsMax** less than the layer thickness. Finally, the **NoEscape** command suppresses an escape file record since the main interest is in the dose distribution.

Figure 27 shows the resulting dose distribution (in Gy) in the steel target after two smoothing cycles. The peak value of 310 rad occurs near a depth of 1.0 cm. The radiation spot has a radius of about 40 mm. For comparison, we can determine the dose without the sweep field. There are two differences in the file **DARHT03.GIN**: 1) substitution of air for the void in the drift region and 2) use of **DARHT\_TOTAL.SRC** in the **SFile** command. The maximum target dose increases to 1300 rad and is concentrated in a 5.0 mm surface layer of the steel plate. The large dose contribution from charged particles is not useful for radiographic applications. For a measurement of the useful dose, it is clearly essential to remove all charged particles.

In the final calculations we shall investigate the feasibility of using a beryllium plate rather than a sweep magnet to remove electrons. The range of 19.8 MeV electrons in solid beryllium is about 62 mm. In the demonstration calculation, a 60 mm block is placed in front of the steel phantom (**DARHT03.MIN**). When the electrons are included (**DARHT04.GIN**), the dose has a strong gradient near the beryllium/steel interface. The value just inside the steel is 326 rad. Removing the electrons and positrons gives the smooth variation of dose shown in Fig. 28. The peak dose in the steel of 280 rad occurs closer to the surface. The implication is that the beryllium shield should be slightly thicker ( $\sim 70.0$  mm) to ensure that electrons and positrons make small contributions.



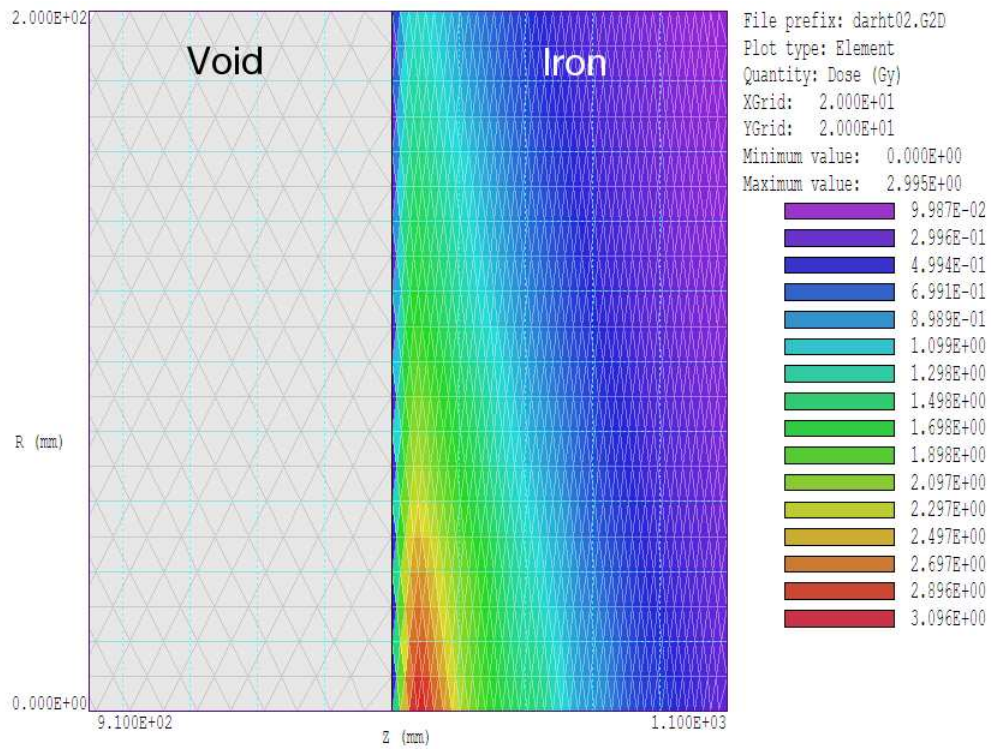


Figure 27: Radiation dose at 1.0 m for the DARHT I beam with a magnetic sweep field.

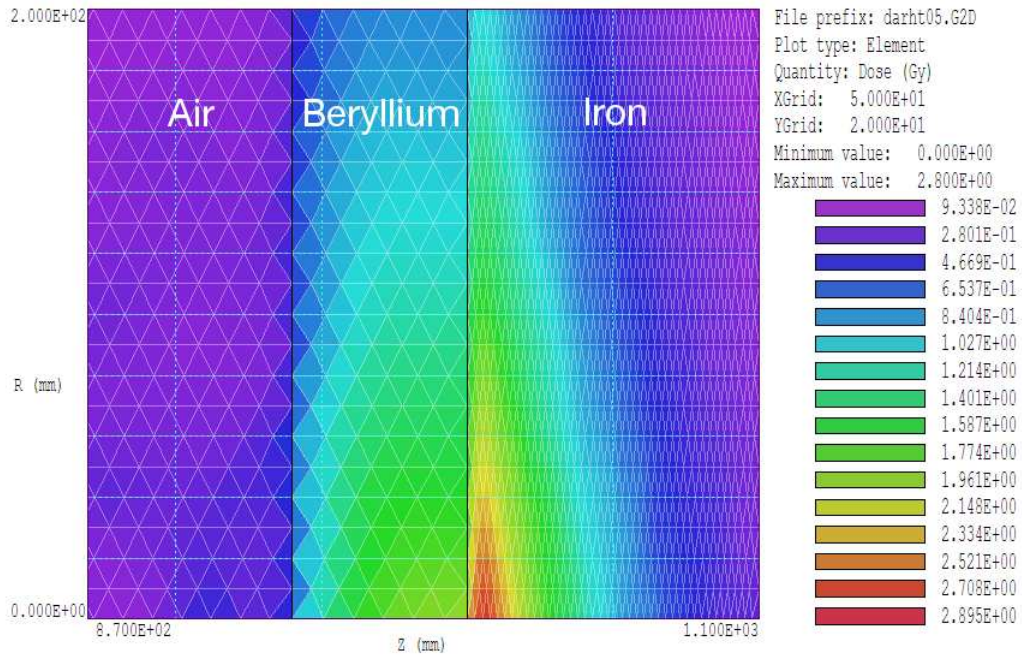


Figure 28: Dose distribution generated by photons for a 60.0 mm beryllium plate in from the steel phantom.



---

## 10 Resolution limits in X-ray radiography

A common issue in X-ray radiography is the ability to resolve small details. Analytic and semi-analytic calculations can give useful results, but often entail simplifying approximations. A full Monte Carlo imaging simulation is computationally intensive and limited by statistical variations. On the other hand, the Monte Carlo approach includes the full effects of the photon energy distributions and scattering. This tutorial illustrates how **GamBet** may be used to find spatial variations of transmitted X-ray flux in the presence of small imperfections. The calculations make extensive use **GenDist** and other available tools in the **GamBet** package.

We shall study propagation of photons in the energy range 600 keV through a steel target. The photons are generated by an ideal point source at an infinite distance. We use a planar two-dimensional geometry to achieve good statistics with moderate run time. The NIST XCom site gives a total attenuation constant for 600 keV photons in iron of  $\mu = 0.61 \text{ cm}^{-1}$ . The scale length for significant photon absorption is on the order of  $1/\mu = 1.65 \text{ cm}$ .

In the calculations, photons move in the  $+x$  direction and enter at  $x = 0.0^+$  cm. In the geometry mesh, Region 1 is iron with thickness along  $x$  of 3.0 cm and Region 2 is a drift space (Void) of length 15.0 cm. The detector is located at the exit plane,  $x = 18.0 \text{ cm}$ . The photon beam has uniform density in  $y$  with a width of 2.0 cm. The first step is to determine the spatial spreading of the photon flux in the detector plane resulting from scattering events. Run **RADIMAGE01** has a single primary photon of energy 600 keV entering a  $y = 0.0$ . The parameter *NPMult* is set so that the run generates 100,000 showers. Figure 29 shows the resulting distribution of transmitted photons in the plane  $x = 18.0 \text{ cm}$  (bin width equals 0.4 mm). The distribution of scattered photons is approximately uniform in  $y$ . The scattered flux is a fraction  $f_s = 3 \times 10^{-3}$  of the primary flux. From this figure, we can estimate a limit on resolution set by photon scattering. Suppose we have a uniform photon beam of width  $W$  incident on the plate and we want to resolve a groove of width  $\delta$ . The fraction of scattered photons over the width of the imperfection is approximately  $F = W f_s / \delta$ . For an imperfection of height 1.0 mm in the 3.0 cm steel plate, the value is  $F = 0.06$ . The groove will be clearly visible if it results in a fractional change of the detector-plane flux equal to or greater than this value.

The series of runs **RADIMAGE02**, **RADIMAGE03** and **RADIMAGE04** addresses resolution limits for illumination with monoenergetic photons. The incident beam has kinetic energy 600 keV with uniform density over a width  $W = 2.0 \text{ cm}$  in  $y$ . As shown in Fig. 30, we introduce a small groove with  $\delta = 1.0 \text{ mm}$  and different depths (5.0, 2.0 and 1.0 mm) and measure the resulting photon flux at the detector plane. It is first necessary to create a distribution of primary photons distributed uniformly in  $y$  between  $\pm 1.0 \text{ cm}$ . We use **GenDist** with the following input file:

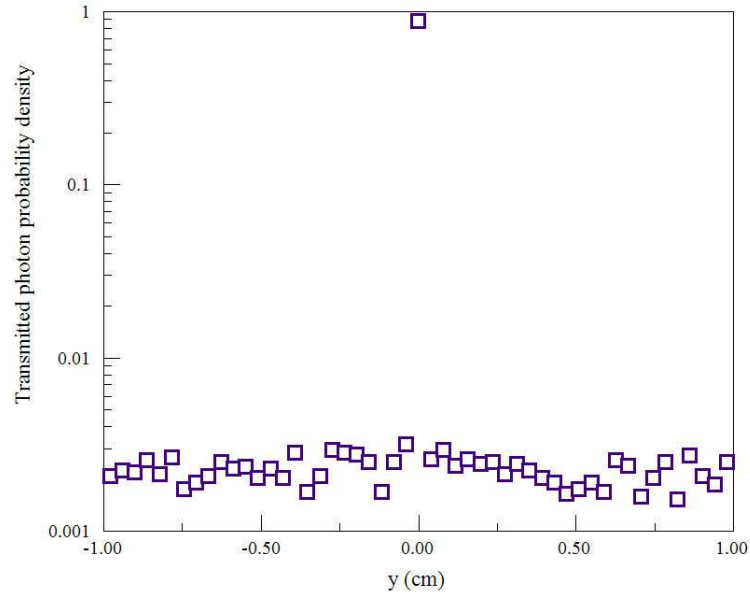


Figure 29: Data from run RADIMAGE01. Photon flux as a function of  $y$  at the detector plane for a point beam injected at  $y = 0.0$  cm. Bin width: 0.4 mm

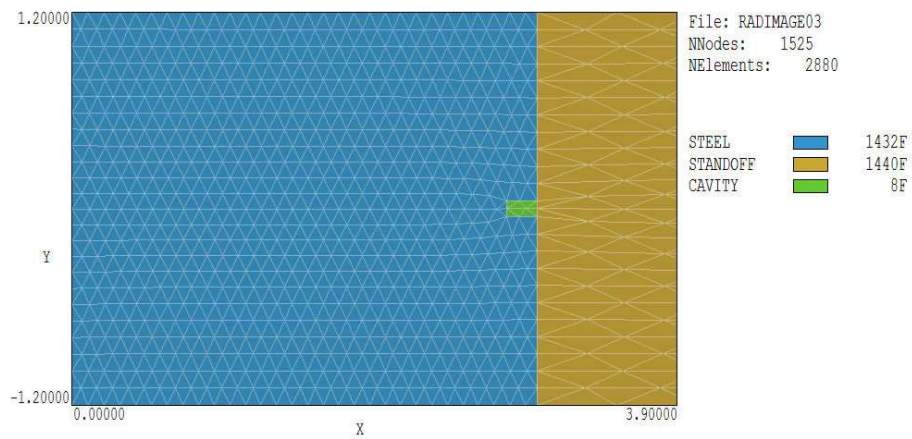


Figure 30: Mesh for run RADIMAGE03. Region 3 represents a groove of width 1.0 mm and depth 2.0 mm on the exit face of the steel plate.

Table 17: Imaging by a monoenergetic photon beam

Pit depth	Attenuation	Prediction	Code
5.0	0.2198	1.354	1.314
2.0	0.1832	1.129	1.140
1.0	0.1725	1.063	1.059
0.0	0.1623	1.000	

```
* GenDist 4.0 Script (Field Precision)
* File: RADIMAGE.DST
FileType = SRC
Particle = P
Energy = 6.0000E+05
Def(Rect) = 0.0000E+00 1.0000E+00 1 20000
Rotate = 0.0000E+00 9.0000E+01 0.0000E+00
Distribution = Uniform
EndFile
```

In response to the script, the program creates the file `RADIMAGE.SRC` with 20,000 particles evenly spaced along  $y$  with direction vectors pointing in  $x$ .

With the parameter value  $NPMult = 25$ , each **GamBet** calculation includes 500,000 showers and takes about 18 minutes on a 3.2 GHz computer. The escape file contains about 360,000 photons. The number drops to 46,000 when a filter is applied that limits photons to the exit plane in the range  $-0.5 \leq y \leq 0.5$ . Figure 31 shows histograms of photon flux in the detector plane with bin width 1.0 mm (equal to the width of the groove) for depths of 5.0 mm, 2.0 mm and 1.0 mm. In all cases, the object is clearly visible over the statistical variations of background flux. The statistical variations of  $\sim \pm 1.6\%$  are consistent with the number of photons per bin,  $N_b \cong 4200$ . The predicted standard deviation is

$$\sigma \cong \frac{1}{\sqrt{N_b}} = 0.0154. \quad (5)$$

Table 17 summarizes the results. The quantity in Column 2 is the attenuation factor,  $\exp(-\mu D)$ . Here,  $D$  is the depth of the plate with the inclusion of the groove. Column 3 shows the predicted signal enhancement as a function of pit depth, determined by taking ratios of quantities in Column 2. Finally, Column 4 shows the code prediction based on the analysis of the results illustrated in Fig. 31.

As a final task, we shall inject a realistic photon energy spectrum to image a groove of depth 2.0 mm. The photons are created by bremsstrahlung interactions of a 1.5 MeV electron beam incident on a tungsten target of thickness 1.4 mm. An initial (SPECTRUM) is performed using a single primary electron with  $NPMult = 10000$  and a bremsstrahlung forcing factor 50.0. Figure 32a shows resulting energy-weighted photon flux emerging from the target in the forward direction. As expected, the distribution approximates a straight-line curve at high energy. The low-energy cutoff is about 0.3 MeV.

For an imaging simulation, we want uniformly distributed photons along  $y$  to form a beam. At all points, the displacement of photon energy from the central value should be assigned with

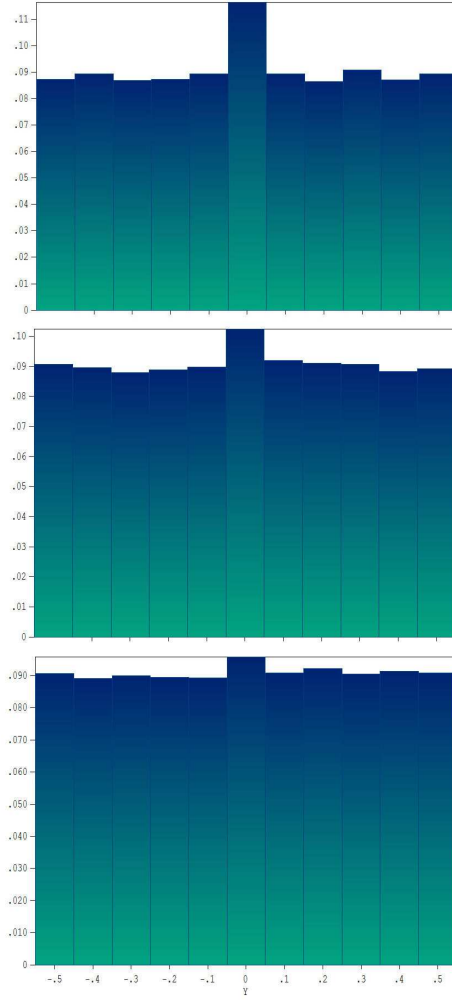


Figure 31: Histograms of photon flux in the detector plane as a function of  $y$  for grooves of width 1.0 mm and depth 5.0 mm (top), 2.0 mm (middle) and 1.0 mm (bottom). Bin width: 1.0 mm

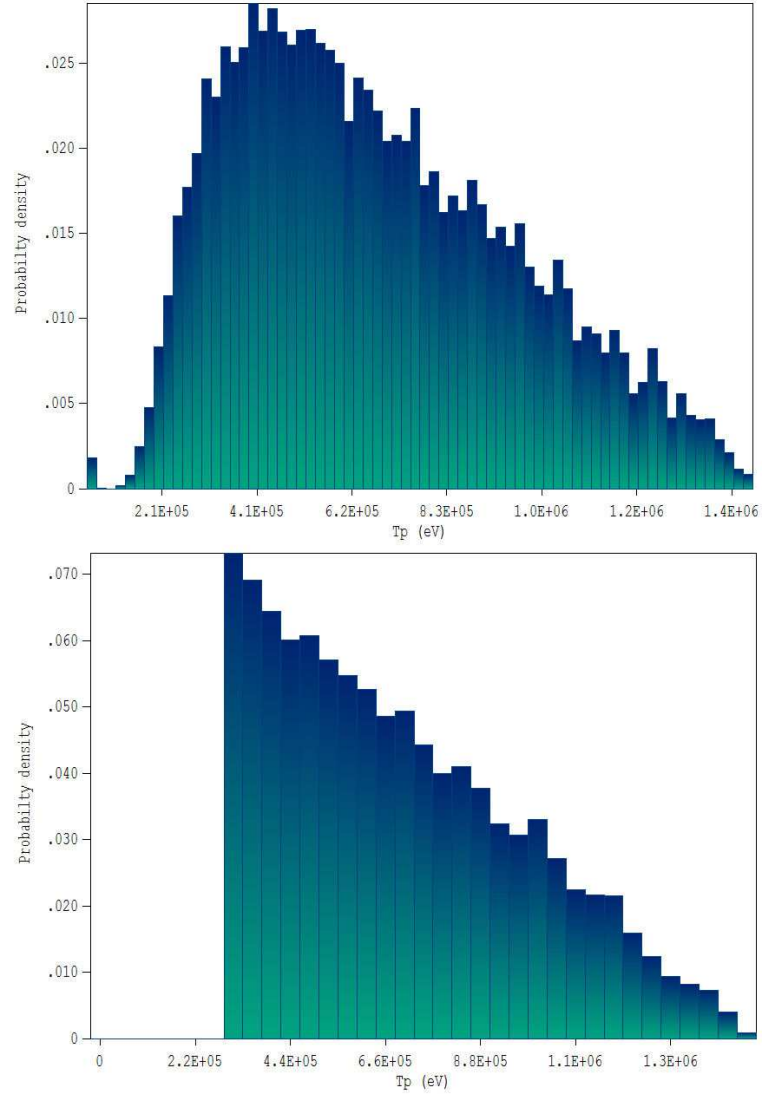


Figure 32: Spectrum of forward-directed bremsstrahlung photons produced by a 1.5 MeV electron beam incident on a 1.4 mm thick tungsten target. Top: GamBet result. Bottom: distribution of electrons injected in RADIMAGE05 from a mathematical approximation.

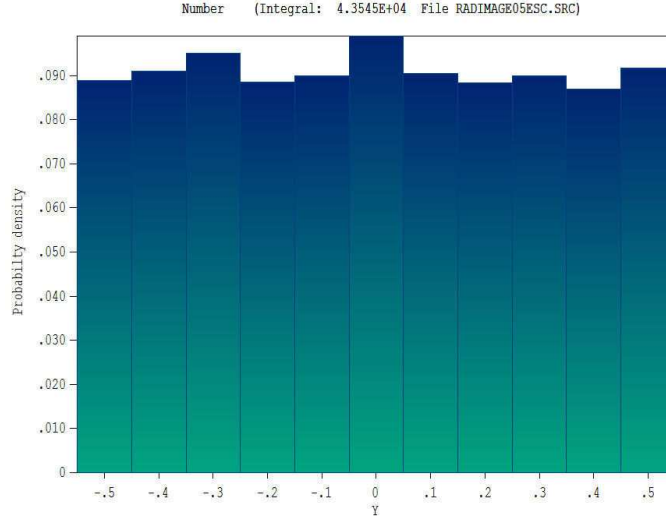


Figure 33: Histogram of photon energy flux in the detector plane as a function of  $y$  for a groove of width 1.0 mm and depth 2.0 mm. The energy of incident photons follows an approximate bremsstrahlung distribution. Bin width: 1.0 mm

weighting to approximate the spectrum of Fig. 32a. One possible approach is to approximate the spectrum by an analytic function, create a table of values using the **Table generator** tool of **GenDist** and then to use the program to create a **SRC** file of incident photons for **GamBet**. As an analytic probability function, we shall use a function that rises sharply to 1.0 at 0.3 MeV and the decreases linearly to zero 0.0 at 1.5 MeV. In this case, the central energy of 0.9 MeV with displacement limits of  $\pm 0.6$  MeV. The following function creates the desired distribution when used in **Table generator** tool of **GenDist**:

$$f(\$x) = 0.25 * (1200000. - ((\$x + 900000) - 300000)) / (\$x + 900000)$$

The results are saved as the file **SPECTRUM**. The file is then used as input to **GenDist** to create the desired distribution in  $y$  and  $T$ . The file **SPECTRUM.DST** has the following content:

```
* GenDist 4.0 Script (Field Precision)
* File: SPECTRUM.DST
FileType = SRC
Particle = P
Energy = 9.0000E+05
Def(Rect) = 0.0000E+00 1.0000E+00 1 20000
Rotate = 0.0000E+00 9.0000E+01 0.0000E+00
Distribution = Random
TDist = Spectrum
EndFile
```

Note the use of random weighting. With uniform weighting, the energy displacement would be correlated with position in  $y$ . The end result is the file **SPECTRUM.SRC** used as input to **RADIMAGE05**.

Figure 32*b* shows the resulting energy flux spectrum of injected photons. Finally, Fig. 33 shows the photon flux distribution in the detector plane after passing through a 3.0 cm steel plate with a groove of width 1.0 mm and depth 2.0 mm. The relative change of photon energy flux is comparable the result of Fig. 31(middle). Statistical variations between bins are somewhat higher with the impressed energy distribution.

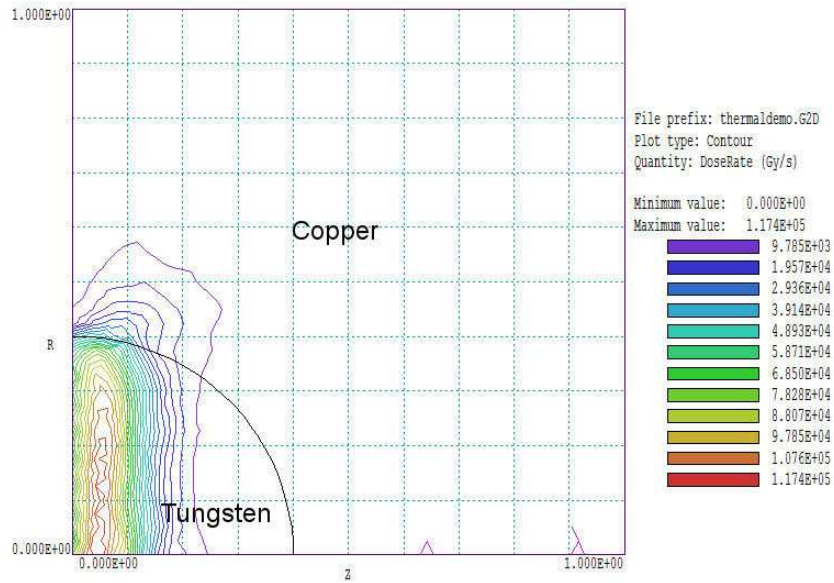


Figure 34: Geometry of the THERMALDOSE example with calculated contours of dose rate. The electron beam is incident on the left-hand boundary.

## 11 Exporting power-density profiles to TDiff

**GamBet** can export data on power deposition in materials for subsequent thermal analysis in **TDiff** and/or **HeatWave**. The benchmark example in this tutorial illustrates solution techniques and a variety of useful features in **GamBet** and **TDiff**. Figure 34 shows a test geometry with cylindrical symmetry. A uniform current-density electron beam with radius 0.4 cm is incident at the left-hand boundary. The beam has kinetic energy 9.0 MeV and current 20.0  $\mu\text{A}$  (corresponding to 180 W incident power). The tungsten target is a hemisphere with radius 0.4 cm. It is embedded in a copper cylinder (radius 1.0 cm, length 1.0 cm) for conductive cooling. Channels at the outer radius of the copper cylinder maintain a fixed temperature of 25.0° C.

The calculations employ the following input files:

- **THERMALDEMO.MIN**. Definition of a mesh applied in both the **GamBet** and **TDiff** calculations. Region 3 is a line region on the outer boundary. It is associated with a fixed-temperature condition for **TDiff**, and ignored by **GamBet** because the program uses only element identities.
- **THERMALDEMO.PRT**. Input file of 100 primary particles to define the electron beam. Model electrons are uniformly distributed in radius with current weighting corresponding to uniform current density. The **Circular beam** tool of the **Trak** program was used to create the file.
- **THERMALDEMO.GIN**. In the **GamBet** script it is necessary to associate all regions with a material; therefore, the nodes of Region 3 are assigned the material properties of copper.



- `THERMALDEMO.TIN`. **TDiff** input file.
- `THERMALMOD.DAT`. Defines a modulation function for **TDiff** to represent the effect of a train of beam pulses.

The first steps are to generate the file `THERMALDOSE.MOU` with **Mesh** and to run the **GamBet** solution. With  $NPMult = 100$ , the code follows 10,000 showers. The code issues a warning in the listing file that Region 3 has zero volume and mass. The calculation is in the *continuous beam* mode (required for export to **TDiff**) because: 1) electron current is specified for the primary particles and 2) the `TPulse` command does not appear. Figure 34 shows the resulting dose-rate distribution. We use the automatic region analysis command in **GBView2** and information in the listing file (`THERMALDOSE.GLS`) to determine the following power-balance quantities:

- Loss to tungsten region: 114.3 W
- Loss to copper region: 21.8 W
- Electron backscatter loss: 10.8 W
- Gamma ray escape: 33.1 W
- Total: 180.0 W

The following command in the **TDiff** script `THERMALDEMO.TIN` loads the **GamBet** dose-rate file:

```
SourceFile = ThermalDemo.G2D
```

In response, **TDiff** loads the dose information, converting it to power density. A scaling factor could be included at the end of the line to investigate different values of beam current. In the thermal calculation, tungsten has the following material properties:  $\rho_w = 1930 \text{ kg/m}^3$ ,  $k_w = 174 \text{ W/m}^\circ\text{C}$  and  $C_{pw} = 130 \text{ J/kg}^\circ\text{C}$ . The corresponding values for copper are  $\rho_c = 892 \text{ kg/m}^3$ ,  $k_c = 401 \text{ W/m}^\circ\text{C}$  and  $C_{pc} = 380 \text{ J/kg}^\circ\text{C}$ . The tungsten target has volume  $1.34 \times 10^{-7} \text{ m}^3$  and mass  $M_w = 2.59 \times 10^{-3} \text{ kg}$ . In the absence of conduction through the copper, the tungsten should heat at the rate

$$\frac{dT}{dt} = \frac{P_w}{M_w C_{pw}} \quad (6)$$

where  $P_w$  represent the power loss of primary and secondary particles in the target. For  $P_w = 114.3 \text{ W}$ , the predicted heating rate is  $340 \text{ }^\circ\text{C/s}$ . If we deactivate heat loss to the copper by setting  $k_c = 0.001$  and  $C_{pc} = 1.0$ , then **TDiff** predicts that the temperature in the target ( $r = 0.0 \text{ cm}$ ,  $z = 0.15 \text{ cm}$ ) rises linearly at a rate  $\sim 350.0 \text{ }^\circ\text{C/s}$ .

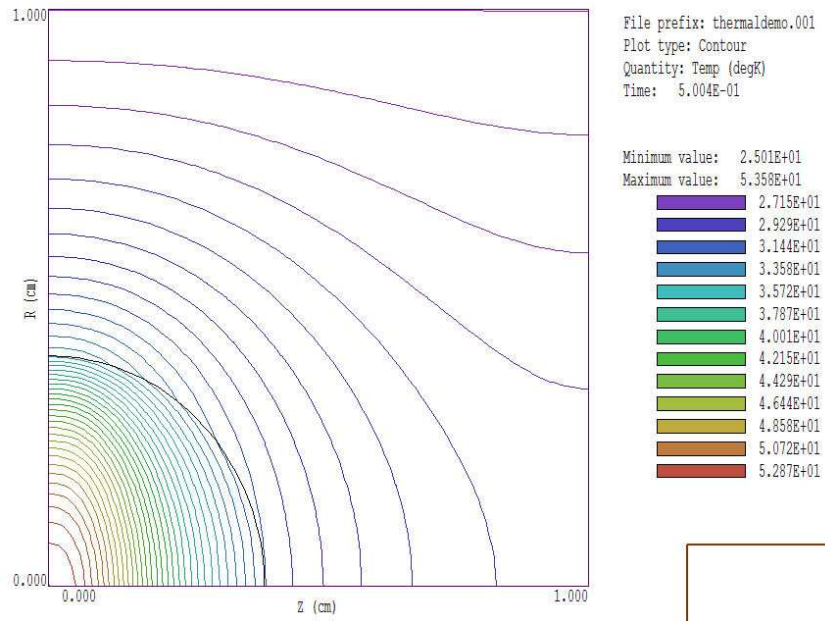


Figure 35: Steady state temperature distribution at  $t = 2.0$  s with a DC beam current.

With the correct material values for copper and constant beam current, **TDiff** gives a solution that reaches 90% of the steady value in 0.21 s. Figure 35 shows temperature contours at 2.0 s. You can also introduce a temporal modulation of the power density to represent, for example, time-variation of the electron beam current. Modulation is initiated with the command:

```
SourceMod = ThermalMod.DAT
```

The file THERMALMOD.DAT defines a pulse train where the beam is off for 0.1 s, on for 0.1 s, and so forth:

```
* File THERMALMOD.DAT
* Pulsed beam On 0.1 s, Off 0.1 s
0.00 0.00
0.09 0.00
0.11 1.00
0.19 1.00
0.21 0.00
0.29 0.00
0.31 1.00
0.39 1.00
0.41 0.00
...
```

Because the function is discontinuous, it is necessary to include the command

```
Interp = Linear
```

in the **TDiff** script. Figure 36 shows the target temperature with the inclusion of beam modulation.

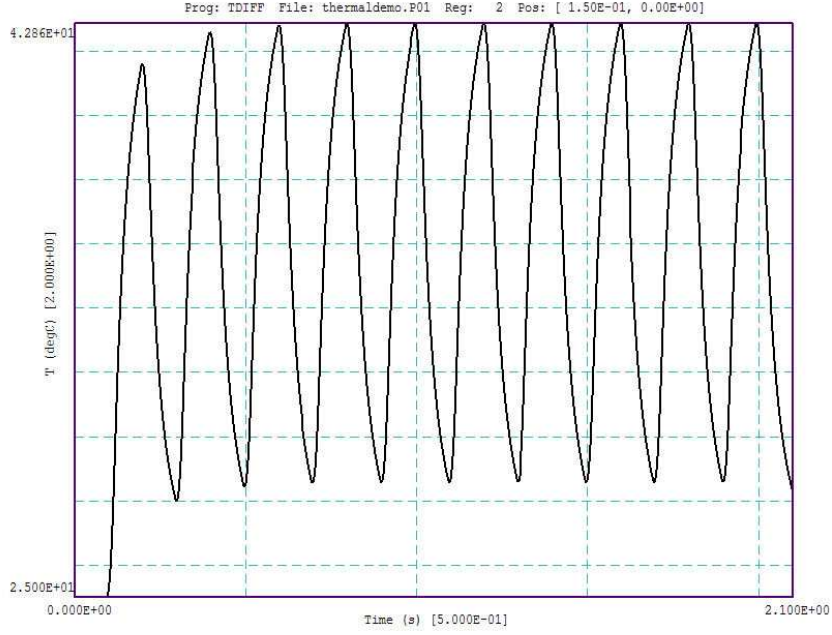


Figure 36: Time variation of temperature in the tungsten target with a train of beam pulses (0.1 s on, 0.1 s off).

## 12 Exporting power-density profiles to HeatWave

This example is similar to the one described in Sect. 11, except that we perform a three-dimensional thermal transport calculation. We shall use an approximately cylindrical geometry for the demonstration to compare the results to a two-dimensional calculation with **TDiff**. Figure 37 shows the configuration. A circular beam of 125 keV electrons is incident on a copper target. The beam has 1.0 mm radius and carries current 50 mA. The **Circular beam** tool of **OmniTrak** was used to create the input file HEATING3D.PRT which contains 613 model electrons.

The mesh of Fig. 37 is defined by the file HEATING3D.MIN. The range of 125 keV electrons in copper is only about 0.036 mm. Because the energy is deposited in a thin layer, we use a fine mesh resolution (0.001 mm) on the target surface. The small elements are required for accuracy in the **HeatWave** calculation but do not influence the **Gambet** calculation.

The file HEATING3D.GIN controls the **Gambet** run to determine the power density distribution. The absorbed power is 5.010 kW compared to the beam power of 6.250 kW. The remaining power is lost through backscattered electrons and photon escape. The backscatter fraction of 0.2889 is close to the measured value for copper (Sect. 1). The **HeatWave** control file HEATING3D.WIN is shown in Table 11. In response to the **SourceFile** command, **HeatWave** reads the **Gambet** output file to define a spatial distribution of power density. The modulation file PULSE250.DAT defines a series of four 250  $\mu$ s pulses at 2.5 ms intervals. The command **Interp linear** is necessary to use the discontinuous step modulation function. The short maximum time step of 2.0  $\mu$ s ensures that the code responds to the modulation function. The command  $NHStep = 10$  limits the history file length to 564 entries.

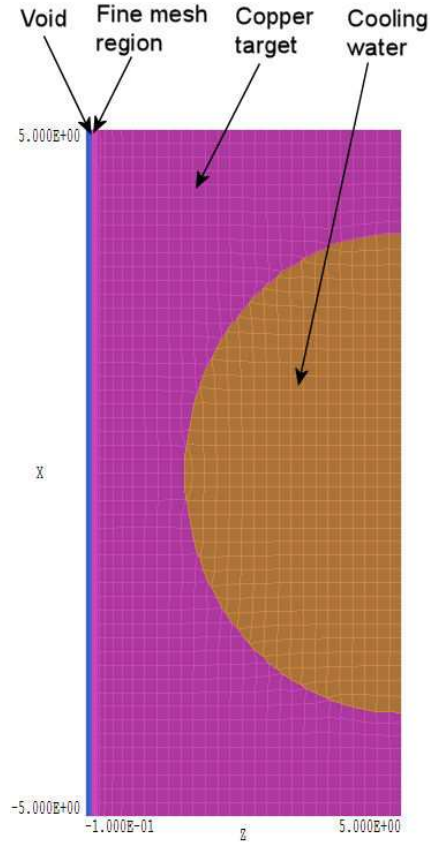


Figure 37: Geometry of the HEATING3D example, dimensions in mm.

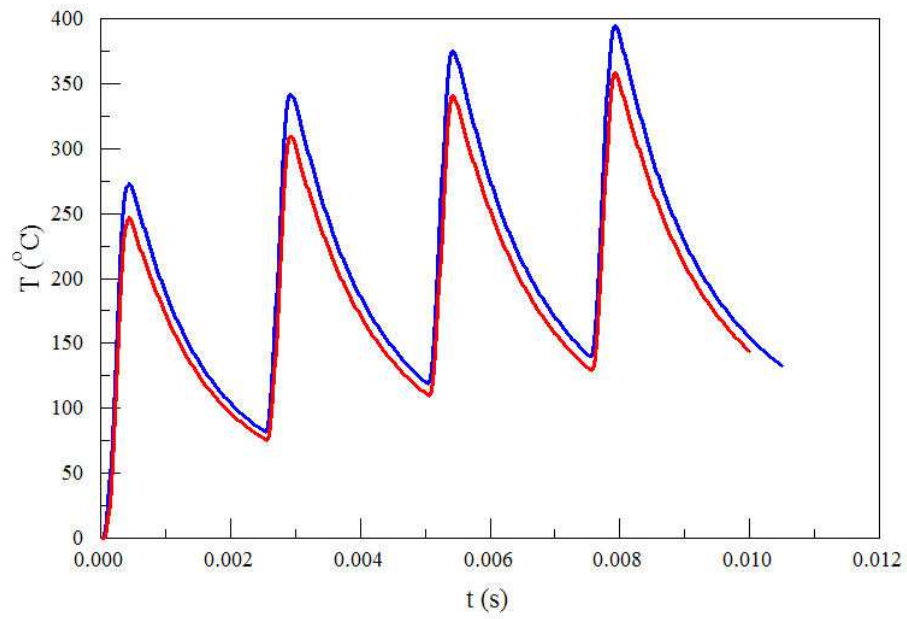


Figure 38: Time-dependent temperature at a point 0.25 mm from the face of the target. Red: **HeatWave** solution (3D). Blue: **TDiff** solution (2D).

Table 18: **HeatWave** input for the HEATING3D example.

```

Mesh = Heating3D
Mode = Dynamic
DUnit = 1.0000E+03
TMax = 1.0500E-02
DtMin = 2.0000E-06
DtMax = 2.0000E-05
Interp Linear
SourceFile = Heating3D.G3D
SourceMod Pulse250.DAT
* Material 1: COPPER
Cond(1) = 386.0
Cp(1) = 387.00
Dens(1) = 8960.0
Init(1) = 25.0
* Material 2: FIXED TEMPERATURE
Fixed(2) = 2.5000E+01
Region(1) = 1
Region(2) = 2
Region(3) = 2
History 0.00 0.00 0.01
History 0.00 0.00 0.25
SetTime 1.0E-4
NHStep = 10
EndFile

```

A probe at location  $z = 0.01$  mm indicates a surface temperature rise of about 860°C during a pulse. The red curve of Fig. 38 is the temperature history at a point 0.25 mm from the surface. For comparison, a two-dimensional cylindrical calculation with **TDiff** gives the blue curve in Fig. 38. For this calculation, **GamBet** predicted a deposited power of 4.969 kW and a backscatter fraction of 0.292.

---

## 13 Electron backscatter at low energy

A conformal mesh offers many advantages in Monte Carlo simulations, but you must exercise some caution when modeling electron backscatter which may take place in a very thin surface layer. Consider determining the transport of backscattered electrons in an X-ray source. The transport calculation involves multiple backscatter generations on multiple surfaces in a system that typically has a scale length on the order of 10 cm. Electrons with kinetic energy 140 keV incident on tungsten have an integrated range of 26  $\mu\text{m}$  and a penetration depth less than 10.0  $\mu\text{m}$ . The disparity in the scale sizes of the system and interaction layer is  $\sim 10000 : 1$ . The implication is that the element size must be much larger than the electron penetration depth for a practical mesh of the full system. In this case, primary electrons that enter material elements remain very close to the surface throughout their complex interactions. With increasing relative element size, it becomes more difficult for a code to determine whether the particles are inside or outside the target material.

The **SCALING** example demonstrates the issues. The three-dimensional calculations determine backscatter of 140 keV electrons on a tungsten target. The **GenDist** input file **SCALING.DST** generates a source file of 2500 model electrons in a rectangular beam with dimensions 8 mm  $\times$  1.8 mm and current 0.25 A. The beam starts in a void region and moves into the target. Backscattered electrons leaving the void region are collected in the escape file for analysis. The target face is inclined  $7^\circ$  with respect to the beam direction to test conformal elements. An initial calculation (**SCALING01**) employs narrow elements of depth 25.0  $\mu\text{m}$ . The output file **SCALING01.GLS** lists a primary escape fraction of 49.1%, consistent with experimental data. The element size is increased to 0.2 mm in the example **SCALING02**. Here, the ratio of the element size to the full penetration depth is greater than 20:1. For this calculation, the computed backscatter ratio drops to 38.5% because of errors in identifying the occupied element for electrons close to the material surface.

The solution to the problem is surprisingly simple and easy to implement: reduce the density of all materials where electron backscatter occurs. The method follows from two facts:

- The relative geometry of the scattering process does not depend on the thickness of the interaction layer as long as the layer depth is small compared to the beam size.
- At reduced density, the probability of interactions is correspondingly lower for electrons entering the material and leaving it.

The implication is that the spatial and energy distribution of backscattered electrons is almost independent of the material density. Reduction of the density increases the thickness of the interaction layer, allowing accurate calculations with larger elements.

You can set non-standard densities using the long form of the **Material** command. For example, this excerpt describes tungsten at one tenth normal density:

```
* 0.1 density tungsten
Material
  Name TungstenLow
  Component 74 1.0
  Density 1.93
  Conductor
End
```

If we reduce the density of tungsten in example **SCALING02** by a factor of 10, the backscatter ratio has the correct value of 49.0%. The average kinetic energy of backscattered electrons is 109.7 keV, close to the value of 109.9 keV from the small element mesh solution. An inspection of the escape files with **GenDist** shows that the backscattered electron distributions are statistically identical for the two calculations.



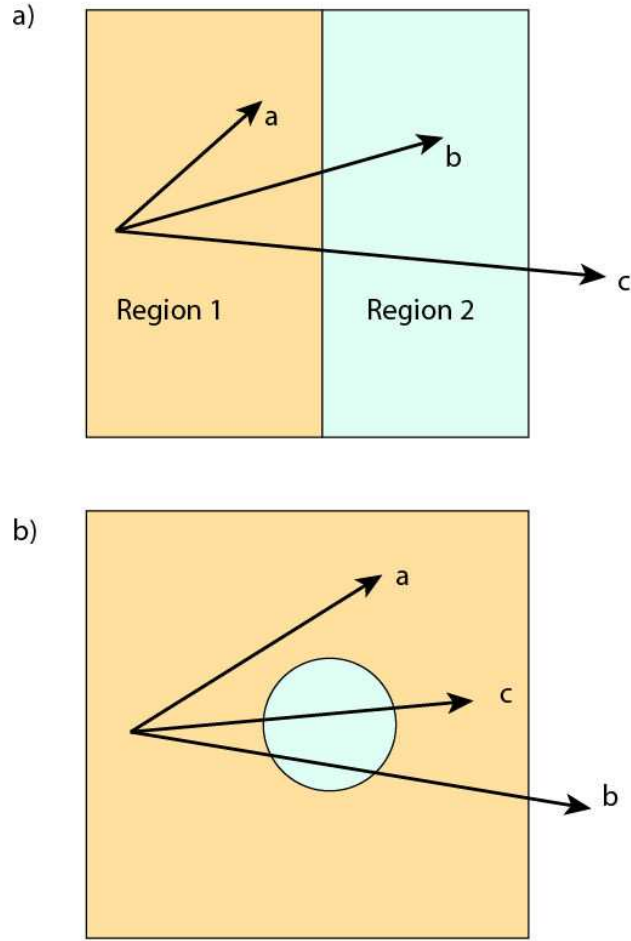


Figure 39: Identifying boundary crossings of gamma rays with a long mean-free-path. *a)* Boundary crossings of photons *b* and *c* are detected. *b)* Boundary crossing of photon *c* is not detected.

## 14 NoStepLimit function in simulations with long-range photons

This tutorial covers the function of the `NoStepLimit` command. The command may speed up runs by reducing operations in photon showers – it should not be used when the solution volume contains isolated structures with size comparable to or less than the gammay-ray mean-free-path. To employ the command, we must understand the interplay between **GamBet** and the **Penelope** routines in the calculation of photon histories.

In the geometry of Fig. 39*a* photons are created at a point in Region 1. Using weighted probability distributions, **Penelope** calculates the distance to the next interaction based on the condition that the particle remains in the same material. If the interaction occurs inside Region 1 (particle *a*), the condition is fulfilled and no special action is required. **Penelope** modifies the

particle parameters to reflect the interaction, and **GamBet** deposits the calculated energy at the interaction point. The case of particle *b* is more complex. The interaction point in Region 2 is not in same material; therefore, the calculated distance to the point is incorrect. On the other hand, we can say with certainty that the photon reaches Region 2 without an interaction. When **GamBet** detects that the interaction point is in different region, the program takes the following actions:

1. Perform a binary search along the vector connecting the start and interaction points to find the region boundary closest to the start point.
2. Move the photon to the boundary point without an interaction.
3. Continue by calculating the next interaction distance using the material properties of Region 2.

The **Penelope** manual<sup>3</sup> shows that this procedure yields correct interaction statistics and energy deposition distributions. The key to the process is detecting when an interaction point is in a different region than the start point. Because the area outside the **GamBet** solution volume is defined as a separate region, the code handles trajectory *b* in Fig. 39a correctly.

Next consider the geometry of Fig. 39b where Region 1 surrounds Region 2. The photon trajectories marked *a* and *b* will be handled correctly, but orbit *c* will cause an error. In this case, **GamBet** does not detect a change of region and therefore does not initiate a boundary search. The error gives skewed statistics and incorrect energy deposition in and around Region 2.

The following two examples illustrate how to detect and to prevent boundary identification errors. The required input files are `STEPLIMIT01.MIN`, `STEPLIMIT01.GIN`, `STEPLIMIT02.MIN` and `STEPLIMIT02.GIN`. The two dimensional calculations have planar geometry. In the example `STEPLIMIT01`, Region 1 is a slab with dimensions 15.0 cm in *x* and *y*. Region 2 is a cylindrical inclusion with radius 3.0 cm. Both regions are assigned the material properties of liquid water in the **GamBet** calculation. A uniform-density sheet beam of 400 keV gamma rays is incident at the left-hand boundary. The beam (consisting of 101 model photons) has width 10.0 cm in *y*. The photons initially move in the *+x* direction. The NIST XCom site gives the following value for the total attenuation coefficient of 400 keV gammays in water:  $\mu = 0.106 \text{ cm}^2/\text{gm} \times 1.0 \text{ gm}/\text{cm}^3 = 0.106 \text{ cm}^{-1}$ . The mean-free path for an interaction is  $\lambda = 1/\mu = 9.43 \text{ cm}$ .

Figure 40 shows deposited energy with activation of the `NoStepLimit` function. The dose exhibits a discontinuity at the region boundary even though there is no difference in material properties. The dose is depressed in Region 2 and enhanced in the downstream section of Region 1. A significant discontinuity of dose at a boundary is a reliable sign of an invalid simulation. The rule holds even at boundaries between different materials because dose from high-energy particles has only a weak dependence on material density.

The problem does not occur in the default mode where the photon step size is artificially limited to ensure detection of boundary crossings. The `DsMax` commands set a maximum step length between interactions of 0.5 cm for both regions. The value is small compared to the 6.0 cm diameter of Region 2. When the `NoStepLimit` command appears, the step limits are applied

---

<sup>3</sup>Francesc Salvat, Jos M. Fernndez-Varea, Josep Sempau, **PENELOPE 2006— A Code System for Monte Carlo Simulation of Electron and Photon Transport** (Workshop Proceedings Barcelona, Spain 4-7 July 2006)

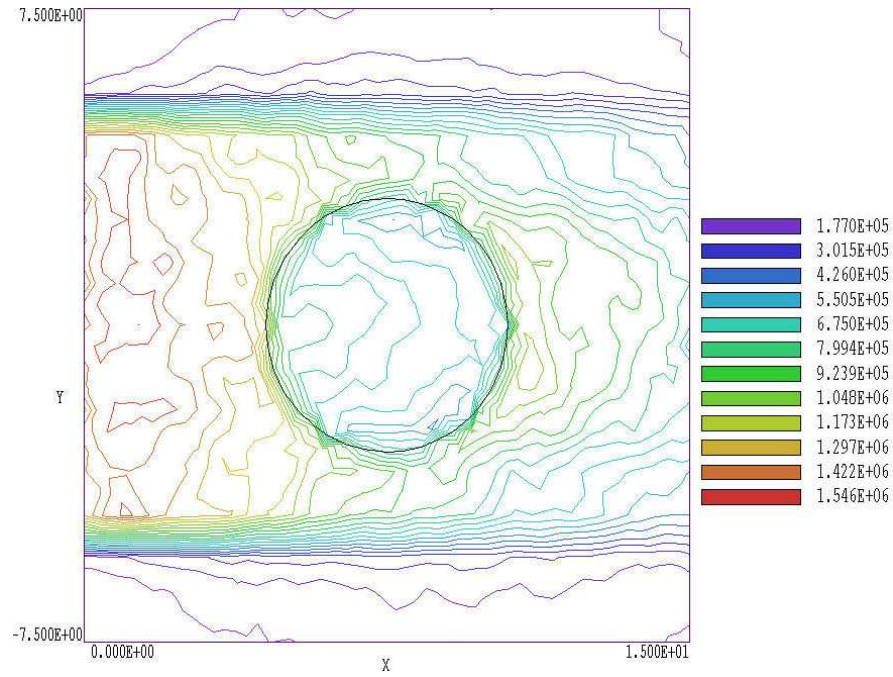


Figure 40: Example STEPLIMIT01, contours of total energy deposition, NoStepLimit command included

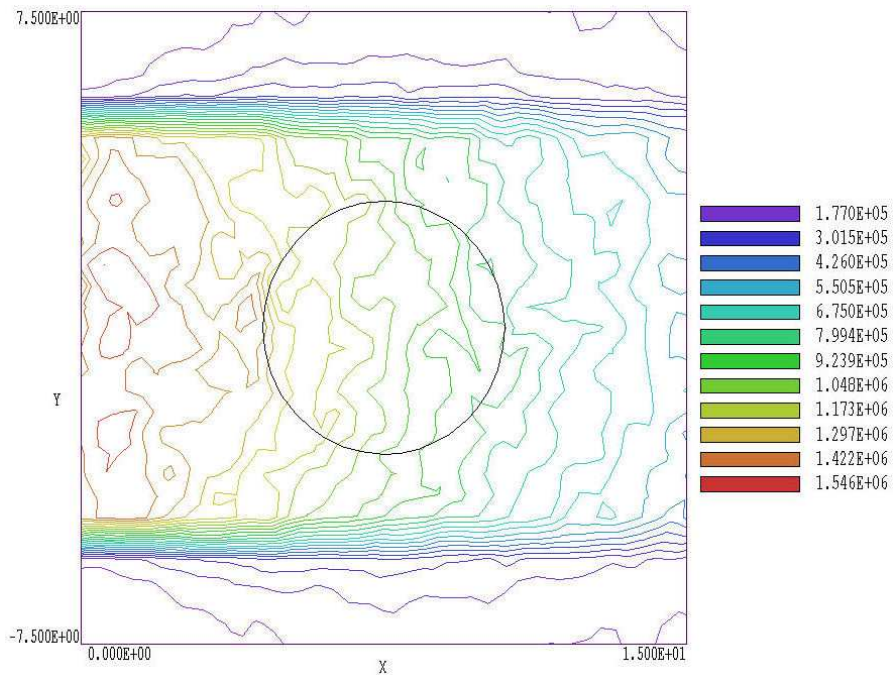


Figure 41: Example STEPLIMIT01, contours of total energy, NoStepLimit command omitted.

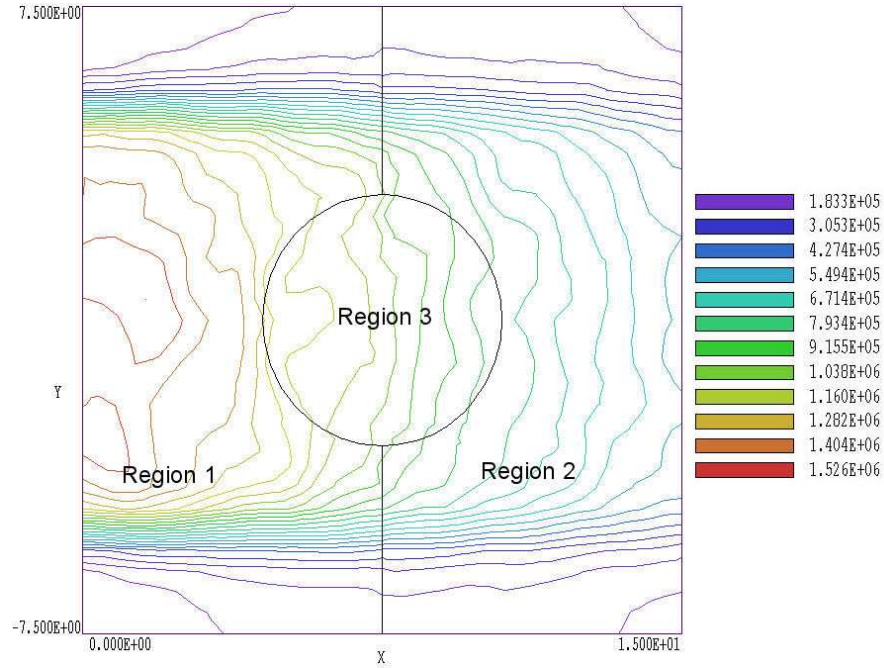


Figure 42: Example STEPLIMIT02, contours of total energy deposition, division of the main region with the NoStepLimit command included.

only to electrons and positrons. The program takes the following actions when the photon step limit is in force: 1) if the distance to the next interaction exceeds  $DsMax$ , move the particle a distance  $DsMax$  without interaction and 2) recalculate the probability of interaction from the new starting point. Although the procedure is somewhat counterintuitive, the **Penelope** manual shows that it preserves the correct statistics and energy deposition distribution. With a limitation on step size, it is almost impossible for a photon to jump over Region 2. Figure 41 shows the dose distribution in the absence of the NoStepLimit command is included. There is no discontinuity at the boundary of Region 2.

The extra work required to enforce the step size limit gives some penalty in run time. The run shown in Fig. 40 required 78 s while the modified run of Fig. 41 required 108 s. You must be alert to the possibility of problems in certain geometries. In simulations with small isolated objects and photons with long mean-free-path, it is a good practice to compare test runs with and without the NoStepLimit command.

We could also resolve the problem by a judicious choice of region boundaries. Figure 42 shows results for example STEPLIMIT02. Here Region 1 has been divided into two regions with the same material properties. It is almost impossible for a photon moving predominantly along  $x$  to traverse Region 3 without entering a different region. As a result, **GamBet** initiates boundary searches for all photons that cross Region 3, independent of the interaction length. Note that the dose in Fig. 42 is continuous across the boundaries, and that the values are consistent with the results of Fig. 41.

Penelope routines used in the program are covered by the following copyright:

PENELOPE/PENGEOM (version 2001) Copyright (c) 2001, Universitat de Barcelona. Permission to use, copy, modify, distribute and sell this software and its documentation for any purpose is hereby granted without fee, provided that the above copyright notice appears in all copies and that both that copyright notice and this permission notice appear in all supporting documentation. The Universitat de Barcelona makes no representations about the suitability of this software for any purpose. It is provided "as is" without express or implied warranty.